

1 Bacterial family-specific enrichment and functions of secretion systems in the rhizosphere

2 A. Fourie^a, J.L. Lopez^{a,b,c}, J.J. Sánchez-Gil^c, S.W.M. Poppeliers^c, R. de Jonge^{cd}, B.E. Dutilh^{a,e}

3 ^aTheoretical Biology and Bioinformatics, Department of Biology, Science for Life, Utrecht University, 3584CH, Utrecht, The
4 Netherlands

5 ^bInstituto de Biotecnología y Biología Molecular, CONICET, CCT-La Plata, Departamento de Ciencias Biológicas, Facultad
6 de Ciencias Exactas, Universidad Nacional de La Plata, La Plata, Argentina

7 ^cPlant-Microbe Interactions, Department of Biology, Science for Life, Utrecht University, 3584CH, Utrecht, The Netherlands

8 ^dAI Technology For Life, Department of Information and Computing Sciences, Science for Life, Utrecht University, 3584CC,
9 Utrecht, The Netherlands

10 ^eInstitute of Biodiversity, Faculty of Biological Sciences, Cluster of Excellence Balance of the Microverse, Friedrich-Schiller-
11 University Jena, 07743, Germany

12

13 Abstract

14 The plant rhizosphere is a highly selective environment where bacteria have developed traits to establish
15 themselves or outcompete other microbes. These traits include bacterial secretion systems (SS's) that
16 range from Type I (T1SS) to Type IX (T9SS) and can play diverse roles. The best known functions are
17 to secrete various proteins or other compounds into the extracellular space or into neighbouring cells,
18 including toxins to attack other microbes or effectors to suppress plant host immune responses. Here,
19 we aimed to determine which bacterial SS's were associated with the plant rhizosphere. We utilised
20 paired metagenomic datasets of rhizosphere and bulk soil samples from five different plant species
21 grown in a wide variety of soil types, amounting to ten different studies. The T3SS and T6SS were
22 generally enriched in the rhizosphere, as observed in studies of individual plant-associated genera. We
23 also identified additional SS's that have received less attention thus far, such as the T2SS, T5SS and
24 *Bacteroidetes*-specific T6SSiii and T9SS. The predicted secreted proteins of some of these systems
25 (T3SS, T5SS and T6SS) could be linked to functions such as toxin secretion, adhesion to the host and
26 facilitation of plant-host interactions (such as root penetration). The most prominent bacterial taxa with
27 rhizosphere- or soil-enriched SS's included *Xanthomonadaceae*, *Oxalobacteraceae*,
28 *Comamonadaceae*, *Caulobacteraceae*, and *Chitinophagaceae*, broadening the scope of known plant-
29 associated taxa that use these systems. We anticipate that the SS's and taxa identified in this study may
30 be utilised for the optimisation of bioinoculants to improve plant productivity.

31

32 **Introduction**

33 Many microbes have symbiotic relationships with plants and are able to colonise the above and below-
34 ground parts of the plant. These plant-associated microbes can act as pathogens, commensals or
35 beneficials. A strong focus for the development of sustainable agriculture has been on utilising plant
36 growth-promoting rhizobacteria (Rosier *et al.*, 2018, Lucke *et al.*, 2020) and biocontrol agents that can
37 contribute directly to plant growth by producing phytohormones (Finkel *et al.*, 2020), facilitating
38 nutrient uptake such as iron, or by producing antibiotics to fend off pathogens (Bakker *et al.*, 2020,
39 Pascale *et al.*, 2020). It is thus essential to understand which microbes are beneficial, how they function
40 and how they can be optimised for agricultural applications (Poppeliers *et al.*, 2023).

41 The root environment is a highly selective environment, influenced by plant root exudates (Pascale *et*
42 *al.*, 2020). This results in a reduced taxonomic diversity closer to the root surface, referred to as the
43 rhizosphere effect (Bakker *et al.*, 2013, Schneijderberg *et al.*, 2020). Near to the plant root, fast-growing
44 microbes are selected (López *et al.*, 2023) that can compete for nutrients and for attachment to the host
45 surface. Other traits that allow bacteria to colonise and persist in the rhizosphere include flagellar
46 motility (Li *et al.*, 2021, López *et al.*, 2023, Sánchez-Gil *et al.*, 2023), attachment and biofilm formation
47 (Seneviratne *et al.*, 2011), processing of plant metabolites (Barret *et al.*, 2011, Sánchez-Gil *et al.*, 2023)
48 and iron chelation (Lemanceau *et al.*, 2009).

49 Bacterial secretion systems (SS's) represent another trait that likely contributes to competition and
50 colonisation in the rhizosphere. These systems include membrane-spanning protein channels that
51 facilitate secretion or translocation of proteins or other molecules that contribute to extracellular nutrient
52 processing, function as effector proteins for host interactions, or as toxins to attack neighbouring
53 microbes (Bernal *et al.*, 2018, Lucke *et al.*, 2020). Known SS's are widely distributed among gram-
54 negative bacteria (Abby *et al.*, 2016, Green *et al.*, 2016), they are prominent among *Proteobacteria* and
55 some other gram-negative phyla and are classified into nine main types, ranging from Type 1 (T1SS)
56 to Type 9 (T9SS). One sub-type of the T6SS, T6SSiii, and the T9SS are restricted to *Bacteroidetes*
57 (James *et al.*, 2022), and a specific T7SS, known as the ESAT-6 SS, is only observed in some genera
58 of the gram-positive *Firmicutes* and *Actinobacteria* phyla (Abdallah *et al.*, 2007, Ates *et al.*, 2016).
59 SS's can be associated to different membranes. In gram negative bacteria, some SS channels are located
60 only in the outer membrane (T2SS, T5SS) while others cross both membranes and some can even
61 penetrate neighbouring bacterial or eukaryotic cells (T3SS, T4SS and T6SS).

62 Distinct functions have been associated with different SS types, based on their secreted proteins. For
63 example, T1SS's contribute to antagonism or host attachment by secretion of toxins or adhesins
64 (Thomas *et al.*, 2014, Hui *et al.*, 2021), T5aSS's and T5cSS's are mostly linked to membrane attachment
65 (Fan *et al.*, 2016) and T5bSS's are involved in contact-dependent growth inhibition (CDI) for
66 interbacterial competition (Willett *et al.*, 2015). T3SS's can suppress host immune responses through

67 translocation of effector proteins (Zboralski *et al.*, 2022) or by contributing to biofilm formation
68 (Castiblanco & Sundin, 2016), and T6SS's secrete toxic effectors intracellularly to attack competing
69 microbes (Gallegos-Monterrosa & Coulthurst, 2021).

70 Functional studies of specific plant-associated bacterial genera support the importance of SS's
71 (including T3SS, T6SS and T7SS) in rhizosphere colonization and survival. In *Pseudomonas*, the T6SS
72 was shown to contribute to interbacterial competition and persistence in the rhizosphere (Bernal *et al.*,
73 2017, Durán *et al.*, 2021, Boak *et al.*, 2022), in *Rhizobium* it played a role in biocontrol (Vogel *et al.*,
74 2021) and in *Xanthomonadales* it contributed to antagonism against prokaryotes and eukaryotes (Bayer-
75 Santos *et al.*, 2019). The T3SS has been shown to facilitate root colonization of legume-associated
76 *Burkholderia* species (Wallner *et al.*, 2021) and for plant growth-promoting *Pseudomonas* strains it can
77 contribute to biocontrol properties or suppression of plant immune responses (Zboralski *et al.*, 2022).
78 Plant-beneficial *Bacilli* utilise T7SS's to secrete a protein that embeds into the plant plasma membrane
79 and causes iron leakage, facilitating root colonization (Liu *et al.*, 2023).

80 Various community-based metagenomic analyses have reported an enrichment in the rhizosphere (vs
81 bulk soil) of some bacterial SS proteins. For example, in cucumber and wheat various genes from the
82 T2SS, T3SS and T6SS were enriched (Ofek-Lalzar *et al.*, 2014), and in barley genes from the T3SS
83 and T6SS were enriched (Bulgarelli *et al.*, 2015). In genome-based comparisons of plant-associated and
84 soil-isolated microbes, T3SS's and T6SS's were also enriched in plant-associated microbes (Levy *et*
85 *al.*, 2018) and specifically in copiotrophs, fast-growing microbes in nutrient-rich environments such as
86 the rhizosphere (López *et al.*, 2023). However, these studies evaluated the different protein components
87 of a SS independently and not as a unit. Except in the case of the T5SS, SS proteins rarely function
88 alone but rather as complexes whose genes occur as operons in the genome. Another challenge for SS
89 analysis is that some proteins can also form part of more than one SS. For example, secretin forms part
90 of the T2SS and the T3SS (Denise *et al.*, 2020) and the gene content of the T6SS and the extracellular
91 contractile injection system (eCIS) are highly similar (Geller *et al.*, 2021). Such functional redundancy
92 can confound abundance estimates of SS's and should be taken into account when interpreting results.

93 To our knowledge, there has not been a comprehensive investigation of all bacterial SS's present in
94 natural root communities of diverse plant species. In addition, the approach of considering all protein
95 components of a SS as a unit to confirm its presence, while excluding redundant proteins, has not been
96 used before, but could impact the detection of prominent SS's. The aim of this study was to determine
97 which SS's were enriched in the rhizosphere environment in comparison to unplanted soil, as an
98 indication of their involvement in rhizosphere colonization and survival. Publicly available metagenome
99 sequencing studies, that evaluated paired rhizosphere and soil samples, were investigated for the
100 presence and abundance of all well-defined bacterial SS's (T1SS-T6SS and T9SS). The studied pairs
101 included diverse plants, i.e. *Arabidopsis thaliana* (two studies), cucumber, wheat, chickpea and various

102 citrus species, allowing us to investigate consistencies between different plant species. In addition to
103 quantifying the SS's, we also assessed their association to bacterial families. Finally, we predicted the
104 secreted proteins of the SS's of interest, including the functional annotation of effector proteins, as an
105 indication of the functional role of the SS's and their contribution to their host bacteria.

106 **Results**

107 **Metagenomic data processing**

108 In this study we utilised existing paired metagenomic datasets of rhizosphere and soil samples, from
109 various plant species (Table S1). This included *Arabidopsis thaliana* (Sanchez-Gil *et al.*, Unpublished,
110 Stringlis *et al.*, 2018), chickpea and wheat (Zhou *et al.*, 2020), citrus species from Brazil, Italy, China
111 and Spain (Xu *et al.*, 2018), and cucumber and wheat (Ofek-Lalzar *et al.*, 2014). The number of raw
112 sequencing reads per dataset ranged from 26M to 115M reads per sample (Table S1), with the datasets
113 from *Arabidopsis* (Stringlis *et al.*, 2018), wheat and cucumber (Ofek-Lalzar *et al.*, 2014) being in the
114 lower range and citrus having the largest datasets (Xu *et al.*, 2018). For ease of reference, these datasets
115 were named as follows: Arabidopsis_Stringlis, Arabidopsis_Sanchez, Chickpea_Zhou, Wheat_Zhou,
116 Cucumber_Ofek, Wheat_Ofek, Citrus_Brazil, Citrus_China, Citrus_Italy, Citrus_Spain. Sequences
117 were quality filtered, host reads removed and then assembled into contigs to allow for gene and protein
118 predictions.

119 The rhizosphere sampling method had a big impact on the number of reads retained after host read
120 removal. In the chickpea and wheat datasets (Zhou *et al.*, 2020) and citrus datasets (Xu *et al.*, 2018)
121 about 97% of the reads were retained as microbial reads whereas for the other studies only 50-60% of
122 the reads were of microbial origin and the remainder were derived from the plant host (see Table S1).
123 In the former studies the soil adhering to the roots was collected and only the soil was used for DNA
124 isolation and sequencing, whereas the other studies included the plant root and the adhering soil. This
125 means that likely more of the tightly-adhering microbes and endophytes were included in the latter
126 studies.

127 The total assembly length varied greatly between datasets, ranging from 72 Mbp in datasets with fewer
128 reads up to 1 Gbp in datasets with the most reads (Table S1). The N50 values of the assemblies also
129 showed an upward trend where datasets with more reads had larger assemblies. However, the
130 *Arabidopsis* datasets had particularly high N50 values, relative to the amount of input reads. This could
131 be an effect of the sampling method and consequently a lower bacterial diversity present in these
132 datasets.

133 The quality of the contigs' assemblies was assessed by the percentage of reads that mapped back to
134 contigs, thus indicating what proportion of the reads were assembled. For most of the datasets an
135 average of 10-20% of the reads mapped to the assembled contigs (Table S1). This low percentage has
136 also been observed in other soil microbiome assemblies and is a result of the high diversity of the soil

137 microbiome. This suggests current algorithms and depth of coverage have a limited resolution to
138 construct inclusive metagenomic assemblies in soil (Howe *et al.*, 2014, Xu *et al.*, 2021).

139 **Rhizosphere sampling methods impact observation of a rhizosphere effect in metagenomes**

140 Previous studies have shown a lower microbial diversity near the root (rhizosphere effect) suggesting
141 stronger selection for specific microbes and functions (Bakker *et al.*, 2013, Schneijderberg *et al.*, 2020).
142 The metagenomic datasets used in this study used different sampling methods, as mentioned earlier.
143 Due to these differences, we wanted to determine if a clear rhizosphere effect could still be observed in
144 all datasets. To this end, we first performed taxonomic read classification of the metagenomic datasets
145 using Kaiju (Menzel *et al.*, 2016). The taxonomic identity could be determined for 82% (± 3.6 SD) of
146 the metagenomic reads of each dataset. Of these, 45% (± 7.1 SD) were classified at the genus rank and
147 51% (± 8.8 SD) at the family rank (Fig. S1). The taxonomic composition and core genera observed in
148 the datasets are summarised in Fig. S2. Using the taxonomic quantification of the reads, we next
149 computed the per-sample alpha diversity at the genus rank, applying the Shannon index that quantifies
150 the number of different organisms and their evenness. This enabled us to compare soil versus
151 rhizosphere alpha diversity per dataset. The alpha diversity was significantly lower in the rhizosphere
152 than in the soil for both *Arabidopsis* datasets, the Citrus_Brazil and the Wheat_Ofek datasets, but
153 significantly higher for the Chickpea_Zhou and the Wheat_Zhou datasets (Fig. 1A; t-test, *p value* <
154 0.05, BH-correction). The other datasets did not show a strong rhizosphere effect either way. The
155 rhizosphere effect was thus predominantly observed in datasets where the root and tightly adhering
156 microbes were included.

157 Visualisation of the beta diversity of the different datasets in a multivariate analysis PCoA plot showed
158 distinct clustering of root and soil samples of most datasets, except Citrus_China and Citrus_Italy (Fig.
159 1B; see Fig. S3 for individual plots). In the combined analysis of all datasets (Fig. 1B), the metagenomic
160 dataset source had the biggest effect on the variation observed, but the interaction between metagenomic
161 dataset and biome (root or soil) was also significant. This suggests some distinct differences between
162 the root and soil communities, per dataset. However, in individual analyses of most datasets the
163 differences were not statistically significant (permanova, *p value* >0.05; Table S2), except for the
164 *Arabidopsis_Sanchez* dataset. This corresponds to the low distinction between biomes and the low
165 rhizosphere effect observed in the alpha diversities.

166 **Four secretion systems showed rhizosphere enrichment in the metagenomic data**

167 Twelve subtypes of well-defined SS's were investigated, including the T1SS - T6SS and T9SS and their
168 respective subtypes (T4SS_I, T4SS_T, T5aSS, T5bSS, T5cSS, T6SS_I, T6SS_{II} and T6SS_{III}). To identify all
169 possible SS structural proteins in the metagenomic datasets and not only those that occurred in
170 assembled contigs, since only 10-20% of the reads were assembled, we used a read mapping approach
171 (see M&M for details). To quantify all the possible SS structural proteins, we first created a

172 comprehensive SS protein database. The first part of this database was created using all 254,090
173 bacterial genomes in the Genome Taxonomy Database (GTDB) (Parks *et al.*, 2021), in order to
174 represent as many taxa as possible. SS's were detected in 129,743 genomes, representing 116 phyla
175 divided into 1,441 families and 4,525 genera (Table S3). Due to the ambiguity of some SS proteins
176 involved in different SS's (see Introduction), a subset of representative proteins was selected per SS. A
177 non-redundant GTDB protein database of 263,396 proteins was created. For each metagenomic dataset
178 a study-specific reference protein database was constructed, consisting of the GTDB SS proteins and
179 those identified in the assembled metagenomic contigs.

180 The DIAMOND blastx algorithm (Buchfink *et al.*, 2015) was used to map metagenomic reads to the
181 SS protein database. Identified proteins were filtered based on percentage sequence identity and
182 percentage coverage of the read mappings. Mapped read counts were converted and normalised similar
183 to transcripts per kilobase million (TPM), but to avoid confusion with RNA transcripts was termed as
184 metagenomic reads per kilobase million (MRPM) in this manuscript.

185 Summaries of the read mapping results confirmed the presence of the T1SS-T3SS, T4SS_T, T5a-cSS,
186 T6SSi, T6SSiii and T9SS in the metagenomic datasets. Some types of SS's were more abundant in the
187 metagenomes than others. The T1SS was the most abundant, followed by T5aSS and T5bSS (Fig. 2).
188 This corresponds to what was observed in the GTDB bacterial genomes (Table S3) where the T1SS,
189 T5aSS and T5bSS were detected in the largest number of bacterial families (765, 542 and 499,
190 respectively), illustrating that some SS's are more widely distributed among bacterial taxa than others.

191 The abundance (MRPM value) of the SS's in the rhizosphere and soil biomes of the different studies
192 were compared to evaluate if there is a higher abundance of specific SS's in one of the two biomes.
193 From a total of 100 comparisons (10 SS's in 10 metagenomic datasets), 20 SS's were significantly
194 enriched in rhizosphere samples and 5 were enriched in soil samples. The remaining 75 comparisons
195 were not significant. All SS's except the T1SS showed enrichment in one or multiple plant datasets
196 (Fig. 2). General trends could be observed across the different datasets; four SS types were more
197 abundant in the rhizosphere in multiple plant host datasets (Fig. 2). This included the T2SS (both
198 *Arabidopsis* sets and *Cucumber_Ofek*), T3SS (both *Arabidopsis* sets, *Cucumber_Ofek* and
199 *Wheat_Zhou*), T5cSS (*Arabidopsis_Sanchez*, *Cucumber_Ofek* and *Wheat_Ofek*) and T6SSi (both
200 *Arabidopsis* sets and *Wheat_Zhou*). The soil-enriched SS's (T4SS_T, T5aSS, T5bSS, T5cSS) were all
201 found in the Zhou datasets, where we also observed an unexpected reverse rhizosphere effect (Fig. 1a).
202 In the latter dataset, the soil was collected from a farm site where different crops have been rotated and
203 soil management included no tillage. This could impact the existing microbial community and perhaps
204 explain the contrasting results observed.

205 **Core bacterial families can be linked to the identified SS's**

206 Based on the Kaiju classification of the metagenomic reads, a total of 559 bacterial families could be
207 identified in the investigated metagenomic datasets. To identify which families in the rhizosphere utilise
208 SS's, and to estimate their abundance, the identified SS proteins were also taxonomically classified up
209 to family rank (see M&M). The number of families in which the different SS's were detected ranged
210 from 267 families (48%) with a T1SS, to 104 – 170 (19% - 30%) with a T3SS, T5SS or T6SSi, to low
211 numbers of 4 (0.7%) and 22 (4%) families with a T6SSiii and T9SS, respectively.

212 The families in which SS's were detected in the majority of the plant datasets ($\geq 80\%$) are of specific
213 interest. These can be considered core families whose members utilise the SS's in different rhizosphere
214 environments. A total of 52 core bacterial families were identified among the metagenomic datasets
215 (Fig. 3). The T1SS was found in the largest number of core bacterial families (37 families), while
216 *Chitinophagaceae* was the only core family in which a T6SSiii and T9SS were consistently detected in
217 all plant studies. Other SS's of interest included the T2SS which was consistent in 10 bacterial families
218 across the plant studies, the T3SS which was found in 18 families and the T6SSi which was identified
219 in 15 families. Since most community-based metagenomic studies primarily focused on functional
220 enrichment and not taxonomic composition of the SS's, this study adds new knowledge on the types of
221 families that may encode for SS's in the rhizosphere. For example, the T3SS's identified in the
222 *Solirubrobacteraceae*, *Bryobacteraceae*, *Oxalobacteraceae* and *Caulobacteraceae* families and the
223 T5bSS's which have, to our knowledge, primarily been identified in plant-associated *Pseudomonas*
224 (Berendsen *et al.*, 2015), *Rhizobium* (Liang *et al.*, 2018) and *Paraburkholderia* (Dias *et al.*, 2019)
225 species.

226 By comparing the total abundance of the different SSs between rhizosphere and soil, many of the SS's
227 were not clearly enriched in either biome (Fig. 2). However, investigating SS abundance per family
228 revealed specific families with enriched SS's in the rhizosphere or soil. A total of 41 families with SS's
229 showed enrichment in multiple plant species (Fig. 4A). If the SS's of the same family are enriched in
230 different plant rhizosphere environments, this suggests it is a common trait in this family and likely
231 plays an important role for some of its species. These families were thus of specific interest.

232 One prominent family was the *Oxalobacteraceae* that was enriched in the rhizosphere in multiple plant
233 datasets for the T3SS, T4SS_T, T5aSS and the T6SS (Fig. 4B). Other families of interest were
234 *Burkholderiaceae* (T3SS, T5SS, T6SS) (Fig. 4B), *Comamonadaceae* (T3SS, T4SS_T, T5SS and T6SSi)
235 (Fig. 4B), *Xanthomonadaceae* (T3SS, T5cSS), *Caulobacteraceae* (T3SS, T5SS and T6SS),
236 *Pseudomonadaceae* (T3SS, T5cSS and T6SS) and some unclassified families in the *Burkholderiales*
237 order. In five of the studies the *Chitinophagaceae* also showed an enrichment of the T6SSiii in the
238 rhizosphere (Fig. 4A).

239 **Functional prediction of SS's in prominent bacterial families - *Arabidopsis thaliana* as model**

240 The aforementioned metagenomic data analyses suggested that SS's were especially important for some
241 of the microbes in the rhizosphere. Next, we focused on predicting the functional roles of these SS's
242 and the potential presence of multiple copies of a SS within a genome. This information cannot be
243 reliably predicted from the metagenomic data, so we constructed a genomic dataset of microbes isolated
244 from the plant rhizosphere. A large collection of 241 genomes is publicly available for *A. thaliana*-
245 associated microbes (referred to as At_microbiome genomes, Table S4, see M&M) and further
246 investigations were thus narrowed to this host. This also allowed identification of the most prominent
247 SS-encoding genera within the families.

248 **The proteins secreted by the T3SS, T5SS and T6SSi facilitate diverse plant and microbe
249 interactions**

250 The prediction of secreted products has most reliably been established for the T3SS, T4SS, T5SS and
251 T6SS (Gerlach & Hensel, 2007, An *et al.*, 2016, Fan *et al.*, 2016, Zeng & Zou, 2017) and predictions
252 were thus restricted to these SS's. The T4SS was excluded, as we focused on those that showed
253 enrichment. The T3SS, T4SS and T6SS directly inject effector proteins into a host cell to interact with
254 host cellular proteins (Galán, 2009), whereas T5SS's also secrete other proteins extracellularly, such as
255 proteases or adhesins. Secreted products were either predicted based on surrounding structural SS genes
256 in the genome, or by blastp comparisons of the proteome to known effectors (for details see M&M).

257 Of the 241 genomes analysed, 62 encoded either one or two copies of a T3SS (Table S5). Based on
258 blastp comparisons of the proteomes to known effectors, a total of 339 putative effectors were identified
259 in these genomes, with a range of 1-13 effectors per genome (average: 5.3 ± 2.3 SD). Proteins with a
260 match were further analysed for secretion signals and eukaryotic-like domains (EffectorT3 model in
261 EffectiveDB; Eichinger *et al.*, 2016). Of the matched proteins, the EffectorT3 model supported 76 and
262 7 as effectors with high (>99%) or medium confidence (>95%), respectively. Some of the prominent
263 domains that were confirmed to occur in effectors in various bacterial families were Shikimate kinase,
264 DUF1512, glycosyl hydrolases and glycosyl transferases, NolW and NolX domains and metallo-beta-
265 lactamase (Fig. S4).

266 The T5aSS, T5bSS and T5cSS were present in 166, 137 and 56 of the At_microbiome genomes,
267 respectively, but the number of copies per genome varied greatly within and between families (Table
268 S6). The highest T5aSS copy number was observed in the genomes of the *Bradyrhizobium* genus in the
269 *Bradyrhizobiaceae* family (4 -12 copies), for T5bSS in unclassified genera in the *Burkholderiaceae* (up
270 to 9 copies) and for T5cSS in the *Variovorax* genus in the *Comamonadaceae* family (up to 8 copies).

271 The T5aSS and T5cSS are autotransporter proteins that code for a transporter domain (anchored in the
272 membrane and facilitating translocation) and a passenger domain which is presented outside the
273 membrane or secreted into the environment (Wilhelm *et al.*, 2011). The most prominent T5aSS
274 passenger domain identified in the genomes was an immunoglobulin (Ig) domain, which was generally

275 present as tandem repeats. This domain has predominantly been associated with host cell attachment,
276 when present on the outer membrane (Luo *et al.*, 2000, Bodelón *et al.*, 2013). Based on the predicted
277 domains, T5aSS's could be divided into different general functional categories, including host cell
278 attachment, membrane hydrolysis, nuclease toxin and various adhesins. The functions differed between
279 genera (Fig. S5A), for example *Variovorax* mostly contained extended signal peptides that contribute
280 to inner membrane translocation (Leyton *et al.*, 2012), *Cupriavidus* had some extended signal peptides
281 but mostly domains for host cell attachment. *Brevudimonas* and *Sphingomonas* had subtilase and
282 acylhydrolase domains, suggesting a role as toxins rather than host attachment in these genera.

283 The T5bSS is a two-partner system where the gene for the transmembrane protein is located next to the
284 secreted protein gene, in the same operon on the genome (Fan *et al.*, 2016). The predominant domains
285 on potential exported proteins were Hemagglutinin domains and MGB/YDG domains, which were
286 generally attached to the Hemagglutinin proteins (Fig. S5B). This protein forms part of the contact-
287 dependent growth inhibition (CDI) system, playing a role in short-range interbacterial competition
288 (Willett *et al.*, 2015). Another prominent domain was a collagen middle domain, identified in genera of
289 the *Burkholderiaceae* family including *Cupriavidus*. Collagen-like bacterial proteins have been linked
290 to attachment and biofilm formation of *Burkholderia* species in animals (Bachert *et al.*, 2015) and
291 attachment to *A. thaliana* roots in a *Bacillus* species (Zhao *et al.*, 2015).

292 T5cSS only contained extended signal peptides and adhesins domains, supporting that these systems
293 solely contribute to cellular adhesion. This system was less prevalent in most of the At_microbiome
294 genomes but had a high copy number in some of the *Burkholderia* (3-5 copies) and *Variovorax* isolates
295 (max 8 copies).

296 The T6SSi was identified in 103 genomes. T6SS effectors can either be attached to the needle tip (cargo
297 effectors) and are thus encoded as an additional domain of this gene in the genome, or will be secreted
298 by the needle structure but are encoded as separate genes which can be found near the needle tip genes
299 (*VgrG/PAAR* or *Hcp*) in the genome. A total of 107 cargo effectors were predicted in the genomes,
300 ranging from one to seven copies per genome. Another 274 other transported effectors were identified,
301 ranging from 1-14 effectors per genome (average: 3.3 ± 3.0 SD). Based on functional domains, the
302 functions predicted for the effectors (corresponding to those previously reported in literature; Table S7)
303 ranged from various anti-bacterial toxins, carboxypeptidase, DNase activity, some eukaryotic targets,
304 membrane pore formation, methyltransferase, peptidoglycan cleavage to post-translational
305 modification (Fig. S6). Proteins with various different DUF domains, with unknown functions but
306 previously associated with effector proteins (see Table S7), were also identified in the genomes. The
307 most abundant effectors were those linked to peptidoglycan cleavage and antibacterial toxins.

308 **Multiple copies of the T6SSi can be placed in different, known, phylogenetic clusters**

309 Multiple copies (2 - 3) of the T6SSi in a single genome were specifically identified in the
310 *Burkholderiaceae*, *Oxalobacteraceae* and *Comamonadaceae* families (Fig. 5; Table S8). The T6SS has
311 been subdivided into five known phylogenetic clusters which can be visualised in phylogenetic trees
312 (Durán *et al.*, 2021). Groups 1, 3 and 4 are commonly found in plant-associated microbes while some
313 others might be predominantly animal-associated. To determine the classification of the different copies
314 of T6SSi's found here, we constructed a phylogenetic tree from all the translated *tssB* genes found in
315 complete T6SSi clusters in the 241 At_microbiome genomes. The T6SS's predominantly grouped into
316 the Group 2, 3 and 4A clusters (Fig. 5).

317 In genomes that had multiple copies of the T6SSi, indicated with coloured labels in Fig. 5, the copies
318 were often in different phylogenetic groups, suggesting complementary functions. For example, two of
319 the copies were in subgroup 3 while the third was in subgroup 4A (*Oxalobacteraceae*) or in 4B
320 (*Comamonadaceae*). This could indicate independent origins of the different copies. Indeed, the
321 effector proteins associated with the different copies also had different functions (Fig. 5). One copy in
322 *Oxalobacteraceae* genomes, for example, was associated with DNase activity, methyltransferase and
323 post-translational modifications, while the second copy only contained *VgrG/Hcp* cargo effectors and
324 proteins linked to peptidoglycan cleavage and the third copy only encoded a *VgrG/Hcp* cargo effector
325 and a protein with a DUF domain previously linked to T6SS effectors.

326 **Four SS's are potentially active in the rhizosphere, based on *A. thaliana* metatranscriptomic 327 data**

328 Metatranscriptomic data were available for the same samples used in the *A. thaliana* metagenomic study
329 (Sanchez-Gil *et al.*, Unpublished). These data were used to determine which SS's were expressed in the
330 soil or rhizosphere. Read mappings were converted to TPM (see M&M). The SS's had a relatively low
331 TPM value compared to those of four housekeeping genes, but active SS's were clear for T1SS, T3SS,
332 T5aSS and T9SS (Fig. S7), with the highest TPM values for T3SS and T5aSS. Expression was detected
333 for eight of the nine core T3SS genes and six of these were significantly enriched (FDR <0.05) in the
334 rhizosphere relative to the soil (logfold 0.7 – 1.8). For the T9SS, seven of the eight core components
335 were expressed and all were more abundant in the rhizosphere (logfold 1.6 – 4.1). Two T6SSi genes,
336 *tssD* and *tssB*, had very high expression levels (Fig. S7). The *tssD* (*Hcp*) gene often occurs
337 independently from the gene cluster, in close proximity to secreted effector proteins or fused to effector
338 proteins and can occur as multiple copies in a genome. This is one explanation for the high expression
339 values. Nonetheless, this gene is considered as a marker to indicate if a T6SS is functional (Bernal *et*
340 *al.*, 2017), suggesting the high levels detected in this study relate to active T6SS's in the rhizosphere.

341 **Discussion**

342 Various bacterial SS's, that are enriched and thus likely contribute to survival in the rhizosphere, were
343 identified in this study. Although several studies have investigated SS's in the genomes of plant-

344 associated bacteria, few have considered their presence in natural root communities (microbiomes) of
345 different plant species (Ofek-Lalzar *et al.*, 2014, Levy *et al.*, 2018). In this multi-plant, comparative
346 metagenomic study, we found that the T2SS, T3SS, T5SS, T6SS and T9SS were more abundant in the
347 rhizosphere community than in bulk soil in at least one plant species. The bacteria encoding these SS's
348 are more abundant near the plant root and likely benefit from the secreted effectors. Enrichment was
349 family-specific and a number of bacterial families were identified that make use of these systems. The
350 potential functions of the SS's were investigated in species of interest, based on the predicted effector
351 proteins, and some prominent functions included a role in interbacterial competition and host cell
352 attachment.

353 Five of the SS types were more abundant in the rhizosphere relative to the bulk soil. Two of these
354 systems, T3SS and T6SS, have received most attention in plant-associated microbiome studies as
355 potential contributors to rhizosphere competence (Bernal *et al.*, 2018, Borrero de Acuña & Bernal,
356 2021, Durán *et al.*, 2021, Zboralski *et al.*, 2022). The current study supports the importance of both
357 these SS's, as they were enriched in three to four different metagenomic datasets. T3SS's also had
358 higher expression levels in the *A. thaliana* rhizosphere than in bulk soil.

359 The collection of effector proteins predicted for T3SS and T6SS paints a picture of the various activities
360 likely occurring simultaneously in such a community. Most predicted T6SS effectors had a toxic effect
361 towards other bacteria that can result in cell lysis or DNA damage. Various *Cupriavidus* species have
362 biocontrol activity against fungi (Ye *et al.*, 2020, Estoppey *et al.*, 2022) and indeed we observed
363 *Cupriavidus* effectors with eukaryotic targets. Functional domains were also identified in T3SS
364 effectors, providing some indication of their role. Functions such as glycosyl hydrolase and glycosyl
365 transferase have been suggested to facilitate plant-microbe interactions (such as root cell penetration)
366 in some genera (Wang *et al.*, 2022) and the NolX domain detected in many effectors can serve as a
367 translocation channel that facilitates transportation of effectors into plant cells (Staehelin & Krishnan,
368 2015). The shikimate kinase domain, present in many of the effectors in the current study, has also been
369 found in a T3SS effector of a *Bradyrhizobium* sp. (Piromyou *et al.*, 2021) and a *Mesorhizobium* sp.
370 (Okazaki *et al.*, 2010). In the latter species one such effector triggered bacterial recognition in the host
371 plant (*Lotus halophilus*) which limited bacterial colonisation and reduced nodulation. Nonetheless, this
372 recognition suggests that this effector domain might also facilitate colonisation of other hosts.

373 Furthermore, additional SS's were identified as important in the rhizosphere, namely T2SS, T5SS,
374 *Bacteroidetes*-specific T6SSiii, and T9SS. T2SS's has mostly been investigated in plant pathogens but
375 also occurs in environmental microbes, facilitating the secretion of CAZymes for cell wall degradation,
376 lipases and proteases that can facilitate plant host colonisation (Cianciotto & White, 2017, Pfeilmeier
377 *et al.*, 2023, Entila *et al.*, 2024). The different T5SS's have rarely been investigated in plant systems
378 but could be big contributors to microbial establishment on the host. In this study, the most abundant

379 functional domain of T5aSS was the Ig domain, associated with host cell attachment (Luo *et al.*, 2000,
380 Bodelón *et al.*, 2013). The T5aSS is well known for its contribution to biofilm formation and adhesion
381 to plant surfaces in some plant-associated microbes (Castiblanco & Sundin, 2016). Its functional
382 importance has been confirmed in *Xanthomonas* pathogens (Alvarez-Martinez *et al.*, 2021) but it has
383 not been studied in other genera. The Hemagglutinin domain was prominent in the T5bSS, a known
384 signature of the contact-dependent growth inhibition (CDI) system. The T5bSS likely also contributes
385 to interbacterial competition or host interaction, as observed in animal hosts (Allen *et al.*, 2020), but
386 this still requires thorough investigation in plant rhizospheres.

387 The rhizosphere-enriched T6SSiii and T9SS were predominantly assigned to members of the
388 *Chitinophagaceae* family, for which the role of their SS's in plant interactions has rarely been
389 investigated. This family is also considered as part of the core microbiome in the rhizosphere and
390 endosphere of different plant species (Schneijderberg *et al.*, 2020). The transcriptomic data from *A.*
391 *thaliana* suggested active expression of the T9SS in the rhizosphere, supporting the involvement of this
392 SS in rhizosphere interactions. T6SSiii plays a similar role as other T6SS's, i.e. producing a needle-like
393 injection structure to attack nearby microbes (Russell *et al.*, 2014), while the T9SS can contribute to
394 gliding motility (i.e. adhesins) and secretion of virulence factors and chitinases (Song *et al.*, 2022).
395 *Chitinophagaceae* genera can be beneficial to plants directly, or serve as biocontrol agents against
396 fungal pathogens (Madhaiyan *et al.*, 2015, Carrión *et al.*, 2019).

397 The enrichment of SS's in the rhizosphere or soil could be linked to various specific bacterial families.
398 Many of these are considered core taxa of plant microbiomes, such as *Rhizobiales*, *Burkholderiales*,
399 *Pseudomonadales*, the *Bacteroidetes* phylum (Banerjee *et al.*, 2018), *Oxalobacteraceae*,
400 *Comamonadaceae* and *Xanthomonadaceae* (Schneijderberg *et al.*, 2020, Johnston-Monje *et al.*, 2021).
401 A predominant focus in studies of T3SS and plant-associated bacteria has been on *Pseudomonas*, root-
402 nodulating *Rhizobiales* and other genera within this order (Stringlis *et al.*, 2019, Wallner *et al.*, 2021,
403 Boak *et al.*, 2022, Zboralski *et al.*, 2022). This study identified additional families likely benefiting
404 from T3SS and T6SS, such as *Oxalobacteraceae*, *Comamonadaceae* and *Caulobacteraceae*. Various
405 genera in these families are considered beneficial microbes (Wen *et al.*, 2020, Berrios, 2021, Yu *et al.*,
406 2021) and could be good candidates for the development of plant growth-promoting microbes or
407 biocontrol agents.

408 The bacterial isolates encoding multiple copies of some SS's were of specific interest, since these copies
409 likely serve complementary functions and provide a larger arsenal of SS tools. This could specifically
410 be investigated in the T6SS, since its corresponding effector genes are located in close proximity to the
411 structural SS genes in the genome. In the *Burkholderiaceae*, *Oxalobacteraceae* and *Comamonadaceae*
412 families, two to three copies were prominent in many isolates. The different copies often grouped in
413 different phylogenetic groups and were linked to different secreted products and functions. Multiple

414 copies have been shown to play different roles in plant growth-promoting microbes. For example, in
415 *Pseudomonas chlororaphis*, two T6SS's contribute to interbacterial competition and protection against
416 predation but the two copies were controlled uniquely and had different bacterial target ranges (Boak
417 *et al.*, 2022). Similarly, in *Pseudomonas putida* three T6SS's were found which collectively contribute
418 to interbacterial competition but one copy was significantly more important for killing a broad range of
419 bacteria than the other two (Bernal *et al.*, 2017).

420 Enriched SS's could not be identified robustly across all the studied datasets. In the *A. thaliana*,
421 cucumber (Ofek-Lalzar *et al.*, 2014) and wheat (Zhou *et al.*, 2020) datasets, various enrichments were
422 observed and the two studies of *A. thaliana* were quite consistent. An explanation for unclear
423 distinctions in the other datasets could be due to the sampling method. In the former studies, the root
424 and tightly adhering bacteria were included whereas in most of the latter studies the root-adhering soil
425 was collected and the root excluded. This can result in smaller differences between the rhizosphere and
426 bulk soil communities. This was also prominent in the alpha diversity differences between rhizosphere
427 and soil communities, where the studies including the root in the sampling displayed a clearer
428 rhizosphere effect (i.e., reduced alpha diversity in the rhizosphere). We thus suggest that alpha and beta
429 diversity measurements should be analysed first and/or used for proper interpretation, as key indicators
430 of the rhizosphere effect.

431 Our comparison of bacterial communities from paired rhizosphere and soil metagenomic samples of
432 different plant hosts revealed an enrichment of many SS's in the rhizosphere, and their functional
433 interpretation highlighted several potential mechanisms by which rhizosphere bacteria might colonize
434 and persist in the rhizosphere. Thus, our study provides a guide of which bacterial families can establish
435 in the rhizosphere, and their SS's that may contribute to this process. Essential functions such as
436 interbacterial competition (T5bSS and T6SS) and attachment to the host surface (T5SS) seem to be
437 important for improving establishment near the root. These SS's can also be transferred to related
438 species of importance to enhance their survival in the rhizosphere environment (Borrero de Acuña &
439 Bernal, 2021). Families with these useful machineries can be mined for additional properties such as
440 plant growth promotion or biocontrol, knowing they have survival benefits in a natural community.

441 **Materials and methods**

442 **Metagenomic data processing and taxonomic composition**

443 Metagenomic sequence data were gathered from publicly available datasets, including paired
444 rhizosphere and soil collections (Ofek-Lalzar *et al.*, 2014, Sanchez-Gil *et al.*, Unpublished, Stringlis *et*
445 *al.*, 2018, Xu *et al.*, 2018, Zhou *et al.*, 2020). Datasets with high quality paired-end Illumina sequence
446 data and at least 30,000 reads per sample were selected for appropriate comparisons between studies.
447 The rhizosphere and soil samples consisted, on average, of three biological replicates. Additional details
448 on the datasets are provided in Table S1.

449 Metagenomic reads were processed, assembled and annotated using the ATLAS pipeline (Kieser *et al.*,
450 2020). Quality filtering included read filtering and trimming based on sequence quality and the removal
451 of host DNA, using appropriate host reference genomes (Table S1). Due to the size of the wheat
452 reference genome an alternative approach was used to remove plant DNA from these datasets, using
453 Kraken 2 (Wood *et al.*, 2019), and only reads that did not match to the eukaryotic database were
454 retained. Metagenome assembly was performed by metaSPAdes (Nurk *et al.*, 2017) and genes were
455 predicted with Prodigal (Hyatt *et al.*, 2010), both included as part of ATLAS. To evaluate the coverage
456 and assembly quality of the metagenomes, the additional step in the ATLAS pipeline was included,
457 where the raw reads were mapped back to the assembly.

458 Taxonomic composition of the metagenomic datasets was determined by read classification, using
459 Kaiju v. 1.6.2 (Menzel *et al.*, 2016). The relative abundances of different genera and families were
460 determined based on all classified bacterial reads. The relative abundances at genus rank were used for
461 calculation of the alpha and beta diversity of the datasets. The Shannon diversity index was calculated
462 as an indication of alpha diversity and differences in alpha diversity between datasets were tested with
463 pairwise t-tests (FDR adjustment Benjamini & Hochberg). For comparison of beta diversity, Bray-
464 Curtis dissimilarity was calculated and differences between datasets were tested with a peranova test,
465 followed by pairwise comparisons with pairwiseAdonis (BH adjustments for FDR). For this analysis
466 genera with relative abundance $>1 \cdot 10^{-5}$ were used. Dataset-specific comparisons between rhizosphere
467 and soil samples of a dataset were also performed using the same approach. Packages used with R 4.0.3
468 (R Core Team, 2020) in RStudio (RStudio Team, 2019) included phyloseq (McMurdie & Holmes,
469 2013), metagMisc (Mikryukov, 2019), vegan v. 2.5-7 (Oksanen *et al.*, 2013) and pairwiseAdonis
470 (Arbizu, 2019).

471 **Identification of secretion systems in the metagenomic data**

472 A read mapping approach was used to identify the SS's in the metagenomes. To create the SS protein
473 database for each metagenomic study, SS proteins were predicted in the metagenomic contigs as well
474 as in the 254,090 GTDB genomes (release 202) (Parks *et al.*, 2021). SS proteins were predicted with
475 MacSyFinder (Abby *et al.*, 2016), which uses an hmm search against the TXSScan models, including
476 the T1SS - T6SS and T9SS and the subtypes T4SS_I, T4SS_T, T5aSS, T5bSS, T5cSS, T6SS_I, T6SS_{II} and
477 T6SS_{III}. In the GTDB genomes, complete SS's were predicted using the gembase mode and in the
478 metagenomes the unordered mode was used. The resulting collection of SS proteins was reduced to a
479 non-redundant set, based on 98% similarity, using CD-hit v. 4.8.1 (Fu *et al.*, 2012). Due to the ambiguity
480 of some components of the SS's (see Introduction), a subset of core genes was selected for many of the
481 SS's (see Table S3) and a DIAMOND BLAST database was generated for downstream analysis
482 (Buchfink *et al.*, 2015).

483 Quality-filtered reads of each metagenome sample were mapped to the SS protein database using the
484 sensitive DIAMOND blastx algorithm (Buchfink *et al.*, 2015) with >40% identity and e-value < 10⁻⁵
485 cut-offs. Results were processed in R Studio to only select genes with >60% coverage and converted to
486 a normalised count, termed metagenomic reads per kilobase million (MRPM). This was based on the
487 formula used for calculating transcripts per kilobase million (TPM), which first normalises for gene
488 length and then for read depth. The term MRPM is used throughout this manuscript to avoid confusion
489 with RNA transcripts. A kingdom-wide study of bacterial SS's indicated that some SS's only occur in
490 specific phyla, such as the T2SS only in *Proteobacteria*, and T6SSiii and T9SS only in Bacteroidetes
491 (Abby *et al.*, 2016). Thus, the MRPM counts were adjusted based on the relative abundance of the phyla
492 known to encode for such SS's (using the formula (MRPM count)/(Phylum relative abundance)). Kaiju
493 analyses of the reads, previously described, were used to determine the relative abundances of the phyla.
494 The MRPM values of all orthologs of each SS gene were summed and the median MRPM value of each
495 SS was determined from all its gene components.

496 For each plant metagenomic dataset, pairwise t-tests were performed to determine which SS's were
497 more abundant in the rhizosphere or the soil biome. Analyses were done in RStudio (RStudio Team,
498 2019), using the rstatix package and *p* values were corrected for FDR (Benjamini-Hochberg).

499 **Taxonomic classification of the identified secretion systems**

500 The SS proteins identified in the metagenomes were classified up to family rank. The SS proteins from
501 the assembled metagenomic contigs were annotated based on CAT classification of the contigs (using
502 NCBI database) (von Meijenfeldt *et al.*, 2019) and those identified on GTDB genomes were annotated
503 based on the GTDB metadata (using NCBI taxonomic names for conformity). The total MRPM value
504 of each SS protein was summed per taxonomic family. To determine the abundance of a SS in a given
505 family, we used an approach similar to pathway predictions in the HUMAnN2 software (Franzosa *et*
506 *al.*, 2018). First, we replaced the lowest MRPM value of a SS protein with that of the second lowest
507 value, as a gap filling approach to compensate for missing proteins or miss-annotation. Second, we
508 calculated the abundance of a SS by averaging the values of all SS proteins in the family (HUMAnN2
509 used average of the top 50% reactions of a pathway). In order to focus mostly on complete SS's in the
510 families, a SS was only included if more than 40% of the proteins were detected for a specific family.

511 Enrichment of the SS's of different families in the rhizosphere or soil were determined with DESeq2
512 v.1.28.1 (Love *et al.*, 2014), using the average calculated MRPM values. A size factor of 1 was used to
513 bypass the normalisation step, since MRPM values were already normalised. Families with SS's that
514 were enriched in the rhizosphere or soil biome in multiple plant species were considered as the families
515 most likely benefitting from the SS's.

516 **Functional prediction of SS's in prominent bacterial families - *Arabidopsis thaliana* as model**

517 More detailed investigations of the secreted protein products were performed on publicly available *A.*
518 *thaliana* isolated genomes (At_microbiome genomes). Genome sources used in this study included
519 IMG (JGI Integrated Microbial Genomes Database; Chen *et al.*, 2022), PATRIC (BV-BRC) database
520 version 2022-02 (Wattam *et al.*, 2017), the At-Sphere collection from the MPIPZ institute (Bai *et al.*,
521 2015) and a local culture collection from Utrecht University, constructed from limed Reijerscamp soil
522 (Selten *et al.*, 2024). Families with SS's that were enriched in the bulk soil or rhizosphere biomes (T2SS,
523 T3SS, T5SS and T6SS) were selected for further analyses, including 241 genomes (Table S4) from the
524 families: *Rhizobiaceae*, *Comamonadaceae*, *Burkholderiaceae*, *Caulobacteraceae*,
525 *Sphingomonadaceae*, *Bradyrhizobiaceae* and *Oxalobacteraceae*.

526 **Prediction of secreted proteins of T3SS, T5SS and T6SS**

527 Secreted proteins were predicted from the previously described At_microbiome genomes resource (Bai
528 *et al.*, 2015, Wattam *et al.*, 2017, Chen *et al.*, 2022, Selten *et al.*, 2024). Functions of putative secreted
529 proteins were predicted by comparison to the Pfam database of protein families (Mistry *et al.*, 2020),
530 using InterProScan v. 5 (Jones *et al.*, 2014).

531 For the T3SS, effector genes are not necessarily located close to the T3SS structural gene cluster in a
532 genome, therefore predictions were based on similarity to verified effector proteins (Hu *et al.*, 2017).
533 The protein sequences from all the genomes with a confirmed T3SS were compared to a previously
534 generated effector database (Hu *et al.*, 2017) using blastp with a >30% identity cutoff. The potential
535 effector proteins were further analysed with the EffectiveT3 model in EffectiveDB (Eichinger *et al.*,
536 2016) for effector signals such as secretion signals and eukaryotic-like domains.

537 T5aSS and T5cSS are autotransporters that encode for a transporter domain and a passenger domain
538 (Wilhelm *et al.*, 2011). The functional annotations of the passenger domains were used to predict the
539 putative functions of the SS's. The T5bSS is a two-partner system where the gene for the outer
540 membrane protein is located next to the secreted protein gene in the same operon on the genome (Fan
541 *et al.*, 2016). Secreted proteins of T5bSS were predicted by collecting all proteins flanking the T5bSS
542 outer membrane protein in the genome. Several functions and domains have been reported in literature
543 for T5bSS (Table S7) (Barret *et al.*, 2011), including contact-dependant growth inhibition (CDI)
544 proteins (Willett *et al.*, 2015, Lin *et al.*, 2020), hemolysins, adhesin proteins, Ig domains (Belikov *et*
545 *al.*, 2021), collagen (Bachert *et al.*, 2015) and tyrosine phosphatase (Rojas-Lopez *et al.*, 2018). Proteins
546 were filtered based on these predicted functions and potential novel functions.

547 The T6SS effectors are often attached to the needle spike protein VgrG or PAAR (C-terminal) and
548 transported as a passenger on the needle tip. Thus the genes of the secreted effectors are either fused,
549 or in close proximity to the *VgrG* or *Hcp* genes on the genome. Putative effectors were predicted by
550 identifying 10 flanking genes on each side of *VgrG* and *Hcp* genes on the genomes and predicting their
551 functional domains. Functional domains that have been associated with T6SS effectors in literature and

552 associated with functions such as peptidoglycan cleavage, nuclease activity, membrane pore formation,
553 interference with energy balance or post-translational modification or various known domains of
554 unknown function (DUF) were used to identify potential effector candidates (Table S7) (Suarez *et al.*,
555 2010, Salomon *et al.*, 2014, Jiang *et al.*, 2016, Klockgether & Tümmler, 2017, Verster *et al.*, 2017,
556 Bayer-Santos *et al.*, 2019, Durán *et al.*, 2021, Jurénas & Journet, 2021, Boak *et al.*, 2022). Predicted
557 secreted proteins smaller than 50 amino acids were excluded from the analysis.

558 **Phylogenetic clusters and copy number of the T6SS's**

559 T6SS's can be subdivided into known phylogenetic clusters, based on the phylogenetic composition of
560 core structural genes. Five clusters have been well-defined in different studies (Group 1-5)(Bernal *et*
561 *al.*, 2018, Durán *et al.*, 2021). To obtain the overall phylogenetic composition of this SS in the
562 *At*_microbiome genomes, the most frequently used phylogenetic marker gene was selected for tree
563 construction (*tssB*). Reference sequences from previous publications were included to easily identify
564 known clusters. Amino acid sequences of the proteins were aligned using MAFFT v 7.453 (Katoh &
565 Standley, 2013), large, gapped regions were removed with trimAl v1.4 (Capella-Gutiérrez *et al.*, 2009),
566 using the heuristic automated setting, and maximum likelihood trees were constructed with IQ-TREE
567 v. 2.1.4 (Minh *et al.*, 2020), including 1000 replicates of ultrafast bootstrap approximations. Trees were
568 visualised and edited in iTOL v.5 (Letunic & Bork, 2021). The number of T6SS's identified in a single
569 genome was also investigated to identify which isolates and genera encode for multiple copies of a
570 T6SS.

571 **Identification of “active” secretion systems in *A. thaliana* metatranscriptomic data**

572 The metatranscriptomic data, from the same samples used in the *A. thaliana* metagenomic study
573 (Sanchez-Gil *et al.*, Unpublished), were used to investigate SS expression. Reads were filtered by
574 removing rRNA sequences using SortMeRNA v. 4.3.4 (Kopylova *et al.*, 2012) and host reads were
575 removed using Kraken 2 (Wood *et al.*, 2019), as described earlier for the metagenomic datasets.
576 Transcriptome assembly was performed with Trinity v. 2.13.2 (Grabherr *et al.*, 2011) with a minimum
577 contig length of 150 bp, a maximum cluster size of 25 was set for the Chrysalis contig clustering step
578 and reads were not normalised. Prediction of coding regions in the assembled transcripts were
579 performed with TransDecoder v. 5.5.0 (Haas, 2023). The second step of CDS prediction with
580 TransDecoder included information on CDSs with hits to the Pfam and Swissprot database as a prior
581 for selecting the best CDSs. A single best CDS was retained per transcript.

582 The identified CDSs were reduced to a non-redundant set (nrCDS) at a 95% similarity threshold using
583 CD-Hit-est (Fu *et al.*, 2012). Reads were mapped to the nrCDS sequences using Bowtie2 (Langmead
584 & Salzberg, 2012) and mapped reads were counted using HtSeq v. 0.11.3 (Putri *et al.*, 2022) with the
585 parameters --nonunique all and --mode union. Read counts were normalised by conversion to transcripts
586 per kilobase million (TPM). All CDSs assigned to the same SS protein were combined for a total count

587 per SS protein and TPM values were compared between the rhizosphere and soil biome samples. Four
588 housekeeping genes (*atpD*, *ftsZ*, *rho* and *rpoA*) were included as a reference indication of the
589 expressions levels that can be obtained for a gene in metatranscriptomic data. Differential expression
590 of each SS protein in the rhizosphere versus the soil were compared with DESeq2 v.1.28.1 (Love *et al.*,
591 2014), using the raw read counts as input.

592 **Data and scripts availability**

593 The scripts used in this study can be accessed at the GitHub repository:
594 https://github.com/Arfourie/Bacterial_SS's. Sequence data from the *A. thaliana* metagenome and
595 metatranscriptome study by Sanchez-Gil *et al.* (Unpublished) will be made available at NCBI SRA
596 upon publication. Genome sequences of isolates from the *A. thaliana* rhizosphere from the UU
597 repository can be accessed at Zenodo (Selten *et al.*, 2024).

598

599

600 **Acknowledgements**

601 This study was supported by the Netherlands Organization for Scientific Research (NWO) Groen II
602 project number ALWGR.2017.002, MiCRop Consortium programme, Harnessing the second genome
603 of plants (Grant number 024.004.014), the European Research Council (ERC) Consolidator grant
604 865694: DiversiPHI, the Deutsche Forschungsgemeinschaft (DFG, German Research Foundation)
605 under Germany's Excellence Strategy – EXC 2051 – Project-ID 390713860, and the Alexander von
606 Humboldt Foundation in the context of an Alexander von Humboldt-Professorship founded by German
607 Federal Ministry of Education and Research.

608

609 **References**

610 Abby SS, Cury J, Guglielmini J, Néron B, Touchon M & Rocha EPC (2016) Identification of protein
611 secretion systems in bacterial genomes. *Scientific Reports* **6**: 23080.

612 Abdallah AM, Gey van Pittius NC, DiGiuseppe Champion PA, Cox J, Luirink J, Vandebroucke-Grauls
613 CMJE, Appelmelk BJ & Bitter W (2007) Type VII secretion — mycobacteria show the way.
614 *Nature Reviews Microbiology* **5**: 883-891.

615 Allen JP, Ozer EA, Minasov G, Shuvalova L, Kiryukhina O, Anderson WF, Satchell KJF & Hauser AR
616 (2020) A comparative genomics approach identifies contact-dependent growth inhibition as a
617 virulence determinant. *Proceedings of the National Academy of Sciences* **117**: 6811-6821.

618 Alvarez-Martinez CE, Sgro GG, Araujo GG, Paiva MRN, Matsuyama BY, Guzzo CR, Andrade MO &
619 Farah CS (2021) Secrete or perish: The role of secretion systems in *Xanthomonas* biology.
620 *Computational and Structural Biotechnology Journal* **19**: 279-302.

621 An Y, Wang J, Li C, Leier A, Marquez-Lago T, Wilksch J, Zhang Y, Webb GI, Song J & Lithgow T
622 (2016) Comprehensive assessment and performance improvement of effector protein predictors
623 for bacterial secretion systems III, IV and VI. *Briefings in Bioinformatics* **19**: 148-161.

624 Arbizu PM (2019) pairwiseAdonis: Pairwise multilevel comparison using adonis R package version
625 0.3. *See* <https://github.com/pmartinezarbizu/pairwiseAdonis>.

626 Ates LS, Houben ENG & Bitter W (2016) Type VII Secretion: A highly versatile secretion system.
627 *Microbiology Spectrum* **4**: 4.1.12.

628 Bachert BA, Choi SJ, Snyder AK, *et al.* (2015) A unique set of the *Burkholderia* collagen-like proteins
629 provides insight into pathogenesis, genome evolution and niche adaptation, and infection
630 detection. *PLOS ONE* **10**: e0137578.

631 Bai Y, Müller DB, Srinivas G, *et al.* (2015) Functional overlap of the *Arabidopsis* leaf and root
632 microbiota. *Nature* **528**: 364-369.

633 Bakker P, Berendsen R, Doornbos R, Wintermans P & Pieterse C (2013) The rhizosphere revisited:
634 root microbiomics. *Frontiers in Plant Science* **4**: 165.

635 Bakker PAHM, Berendsen RL, Van Pelt JA, *et al.* (2020) The soil-borne identity and microbiome-
636 assisted agriculture: Looking back to the future. *Molecular Plant* **13**: 1394-1401.

637 Banerjee S, Schlaepi K & van der Heijden MGA (2018) Keystone taxa as drivers of microbiome
638 structure and functioning. *Nature Reviews Microbiology* **16**: 567-576.

639 Barret M, Morrissey JP & O'Gara F (2011) Functional genomics analysis of plant growth-promoting
640 rhizobacterial traits involved in rhizosphere competence. *Biology and Fertility of Soils* **47**: 729-
641 743.

642 Bayer-Santos E, de Moraes Ceseti L, Farah CS & Alvarez-Martinez CE (2019) Distribution, function
643 and regulation of Type 6 secretion systems of Xanthomonadales. *Frontiers in Microbiology* **10**:
644 458221.

645 Belikov SI, Petrushin IS & Chernogor LI (2021) Genome Analysis of the *Janthinobacterium* sp. Strain
646 SLB01 from the Diseased Sponge of the *Lubomirskia baicalensis*. *Current Issues in Molecular
647 Biology* **43**: 2220-2237.

648 Berendsen RL, van Verk MC, Stringlis IA, Zamioudis C, Tommassen J, Pieterse CMJ & Bakker PAHM
649 (2015) Unearthing the genomes of plant-beneficial *Pseudomonas* model strains WCS358,
650 WCS374 and WCS417. *BMC Genomics* **16**: 539.

651 Bernal P, Llamas MA & Filloux A (2018) Type VI secretion systems in plant-associated bacteria.
652 *Environmental Microbiology* **20**: 1-15.

653 Bernal P, Allsopp LP, Filloux A & Llamas MA (2017) The *Pseudomonas putida* T6SS is a plant warden
654 against phytopathogens. *The ISME Journal* **11**: 972-987.

655 Berrios L (2021) Plant-growth-promoting *Caulobacter* strains isolated from distinct plant hosts share
656 conserved genetic factors involved in beneficial plant–bacteria interactions. *Archives of
657 Microbiology* **204**: 43.

658 Boak EN, Kirolos S, Pan H, Pierson LS & Pierson EA (2022) The Type VI secretion systems in plant-
659 beneficial bacteria modulate prokaryotic and eukaryotic interactions in the rhizosphere.
660 *Frontiers in Microbiology* **13**: 843092.

661 Bodelón G, Palomino C & Fernández LÁ (2013) Immunoglobulin domains in *Escherichia coli* and
662 other enterobacteria: from pathogenesis to applications in antibody technologies. *FEMS
663 Microbiology Reviews* **37**: 204-250.

664 Borrero de Acuña JM & Bernal P (2021) Plant holobiont interactions mediated by the type VI secretion
665 system and the membrane vesicles: promising tools for a greener agriculture. *Environmental
666 Microbiology* **23**: 1830-1836.

667 Buchfink B, Xie C & Huson DH (2015) Fast and sensitive protein alignment using DIAMOND. *Nature
668 Methods* **12**: 59-60.

669 Bulgarelli D, Garrido-Oter R, Münch Philipp C, Weiman A, Dröge J, Pan Y, McHardy Alice C &
670 Schulze-Lefert P (2015) Structure and function of the bacterial root microbiota in wild and
671 domesticated barley. *Cell Host & Microbe* **17**: 392-403.

672 Capella-Gutiérrez S, Silla-Martínez JM & Gabaldón T (2009) trimAl: a tool for automated alignment
673 trimming in large-scale phylogenetic analyses. *Bioinformatics* **25**: 1972-1973.

674 Carrión VJ, Perez-Jaramillo J, Cordovez V, *et al.* (2019) Pathogen-induced activation of disease-
675 suppressive functions in the endophytic root microbiome. *Science* **366**: 606-612.

676 Castiblanco LF & Sundin GW (2016) New insights on molecular regulation of biofilm formation in
677 plant-associated bacteria. *Journal of Integrative Plant Biology* **58**: 362-372.

678 Chen I-MA, Chu K, Palaniappan K, *et al.* (2022) The IMG/M data management and analysis system
679 v.7: content updates and new features. *Nucleic Acids Research* **51**: D723-D732.

680 Cianciotto NP & White RC (2017) Expanding Role of Type II Secretion in Bacterial Pathogenesis and
681 Beyond. *Infection and Immunity* **85**: e00014-00017.

682 Denise R, Abby SS & Rocha EPC (2020) The Evolution of Protein Secretion Systems by Co-option
683 and Tinkering of Cellular Machineries. *Trends in Microbiology* **28**: 372-386.

684 Dias GM, de Sousa Pires A, Grilo VS, Castro MR, de Figueiredo Vilela L & Neves BC (2019)
685 Comparative genomics of *Paraburkholderia kururiensis* and its potential in bioremediation,
686 biofertilization, and biocontrol of plant pathogens. *MicrobiologyOpen* **8**: e00801.

687 Durán D, Bernal P, Vazquez-Arias D, Blanco-Romero E, Garrido-Sanz D, Redondo-Nieto M, Rivilla
688 R & Martín M (2021) *Pseudomonas fluorescens* F113 type VI secretion systems mediate
689 bacterial killing and adaption to the rhizosphere microbiome. *Scientific Reports* **11**: 5772.

690 Eichinger V, Nussbaumer T, Platzer A, Jehl MA, Arnold R & Rattei T (2016) EffectiveDB--updates
691 and novel features for a better annotation of bacterial secreted proteins and Type III, IV, VI
692 secretion systems. *Nucleic Acids Res* **44**: D669-674.

693 Entila F, Han X, Mine A, Schulze-Lefert P & Tsuda K (2024) Commensal lifestyle regulated by a
694 negative feedback loop between *Arabidopsis* ROS and the bacterial T2SS. *Nature
695 Communications* **15**: 456.

696 Estoppey A, Weisskopf L, Di Francesco E, Vallat-Michel A, Bindschedler S, Chain PS & Junier P
697 (2022) Improved methods to assess the effect of bacteria on germination of fungal spores.
698 *FEMS Microbiology Letters* **369**: fnac034.

699 Fan E, Chauhan N, Uddatha DBRKG, Leo JC & Linke D (2016) Type V secretion systems in bacteria.
700 *Microbiology Spectrum* **4**: 4.1.10.

701 Finkel OM, Salas-González I, Castrillo G, Conway JM, Law TF, Teixeira PJPL, Wilson ED, Fitzpatrick
702 CR, Jones CD & Dangl JL (2020) A single bacterial genus maintains root growth in a complex
703 microbiome. *Nature* **587**: 103-108.

704 Franzosa EA, McIver LJ, Rahnavard G, *et al.* (2018) Species-level functional profiling of metagenomes
705 and metatranscriptomes. *Nature Methods* **15**: 962-968.

706 Fu L, Niu B, Zhu Z, Wu S & Li W (2012) CD-HIT: accelerated for clustering the next-generation
707 sequencing data. *Bioinformatics* **28**: 3150-3152.

708 Galán JE (2009) Common themes in the design and function of bacterial effectors. *Cell Host Microbe*
709 5: 571-579.

710 Gallegos-Monterrosa R & Coulthurst SJ (2021) The ecological impact of a bacterial weapon: microbial
711 interactions and the Type VI secretion system. *FEMS Microbiology Reviews* 45: fuab033.

712 Geller AM, Pollin I, Zlotkin D, Danov A, Nachmias N, Andreopoulos WB, Shemesh K & Levy A
713 (2021) The extracellular contractile injection system is enriched in environmental microbes and
714 associates with numerous toxins. *Nature Communications* 12: 3743.

715 Gerlach RG & Hensel M (2007) Protein secretion systems and adhesins: The molecular armory of
716 Gram-negative pathogens. *International Journal of Medical Microbiology* 297: 401-415.

717 Grabherr MG, Haas BJ, Yassour M, *et al.* (2011) Full-length transcriptome assembly from RNA-Seq
718 data without a reference genome. *Nat Biotechnol* 29: 644-652.

719 Green ER, Mecsas J & Kudva IT (2016) Bacterial secretion systems: An overview. *Microbiology*
720 *Spectrum* 4: 4.1.13.

721 Haas BJ (2023) TransDecoder V.5, <https://github.com/TransDecoder/TransDecoder>.

722 Howe AC, Jansson JK, Malfatti SA, Tringe SG, Tiedje JM & Brown CT (2014) Tackling soil diversity
723 with the assembly of large, complex metagenomes. *Proceedings of the National Academy of*
724 *Sciences* 111: 4904-4909.

725 Hu Y, Huang H, Cheng X, Shu X, White AP, Stavrinides J, Köster W, Zhu G, Zhao Z & Wang Y (2017)
726 A global survey of bacterial type III secretion systems and their effectors. *Environmental*
727 *Microbiology* 19: 3879-3895.

728 Hui X, Chen Z, Zhang J, Lu M, Cai X, Deng Y, Hu Y & Wang Y (2021) Computational prediction of
729 secreted proteins in gram-negative bacteria. *Computational and Structural Biotechnology*
730 *Journal* 19: 1806-1828.

731 Hyatt D, Chen G-L, LoCascio PF, Land ML, Larimer FW & Hauser LJ (2010) Prodigal: prokaryotic
732 gene recognition and translation initiation site identification. *BMC Bioinformatics* 11: 119.

733 James RH, Deme JC, Hunter A, Berks BC & Lea SM (2022) Structures of the Type IX
734 Secretion/Gliding Motility Motor from across the Phylum *Bacteroidetes*. *mBio* 13: e00267-
735 00222.

736 Jiang F, Wang X, Wang B, Chen L, Zhao Z, Waterfield NR, Yang G & Jin Q (2016) The *Pseudomonas*
737 *aeruginosa* Type VI Secretion PGAP1-like Effector Induces Host Autophagy by Activating
738 Endoplasmic Reticulum Stress. *Cell Reports* 16: 1502-1509.

739 Johnston-Monje D, Gutiérrez JP & Lopez-Lavalle LAB (2021) Seed-transmitted bacteria and fungi
740 dominate juvenile plant microbiomes. *Frontiers in Microbiology* 12: 737616.

741 Jones P, Binns D, Chang H-Y, *et al.* (2014) InterProScan 5: genome-scale protein function
742 classification. *Bioinformatics* 30: 1236-1240.

743 Jurénas D & Journet L (2021) Activity, delivery, and diversity of Type VI secretion effectors. *Molecular*
744 *Microbiology* 115: 383-394.

745 Katoh K & Standley DM (2013) MAFFT multiple sequence alignment software version 7:
746 improvements in performance and usability. *Mol Biol Evol* **30**: 772-780.

747 Kieser S, Brown J, Zdobnov EM, Trajkovski M & McCue LA (2020) ATLAS: a Snakemake workflow
748 for assembly, annotation, and genomic binning of metagenome sequence data. *BMC
749 Bioinformatics* **21**: 257.

750 Klockgether J & Tümmeler B (2017) Recent advances in understanding *Pseudomonas aeruginosa* as a
751 pathogen. *F1000Research* **6**: 1261.

752 Kopylova E, Noé L & Touzet H (2012) SortMeRNA: fast and accurate filtering of ribosomal RNAs in
753 metatranscriptomic data. *Bioinformatics* **28**: 3211-3217.

754 Langmead B & Salzberg SL (2012) Fast gapped-read alignment with Bowtie 2. *Nature Methods* **9**: 357-
755 359.

756 Lemanceau P, Expert D, Gaymard F, Bakker PAHM & Briat JF (2009) Chapter 12 Role of Iron in
757 Plant–Microbe Interactions. *Advances in Botanical Research*, Vol. 51 p. 491-549. Academic
758 Press.

759 Letunic I & Bork P (2021) Interactive Tree Of Life (iTOL) v5: an online tool for phylogenetic tree
760 display and annotation. *Nucleic Acids Research* **49**: W293-W296.

761 Levy A, Salas Gonzalez I, Mittelviefhaus M, *et al.* (2018) Genomic features of bacterial adaptation to
762 plants. *Nature Genetics* **50**: 138-150.

763 Leyton DL, Rossiter AE & Henderson IR (2012) From self sufficiency to dependence: mechanisms and
764 factors important for autotransporter biogenesis. *Nature Reviews Microbiology* **10**: 213-225.

765 Li E, Zhang H, Jiang H, Pieterse CMJ, Jousset A, Bakker PAHM & de Jonge R (2021) Experimental-
766 evolution-driven identification of *Arabidopsis* rhizosphere competence genes in *Pseudomonas
767 protegens*. *mBio* **12**: e00927-00921.

768 Liang J, Hoffrichter A, Brachmann A & Marín M (2018) Complete genome of *Rhizobium
769 leguminosarum* Norway, an ineffective Lotus micro-symbiont. *Standards in Genomic Sciences*
770 **13**: 36.

771 Lin H-H, Filloux A & Lai E-M (2020) Role of Recipient Susceptibility Factors During Contact-
772 Dependent Interbacterial Competition. *Frontiers in Microbiology* **11**: 603652.

773 Liu Y, Shu X, Chen L, *et al.* (2023) Plant commensal type VII secretion system causes iron leakage
774 from roots to promote colonization. *Nature Microbiology* **8**: 1434-1449.

775 López JL, Fourie A, Poppeliers SWM, Pappas N, Sánchez-Gil JJ, de Jonge R & Dutilh BE (2023)
776 Growth rate is a dominant factor predicting the rhizosphere effect. *The ISME Journal* **17**: 1396-
777 1405.

778 Love MI, Huber W & Anders S (2014) Moderated estimation of fold change and dispersion for RNA-
779 seq data with DESeq2. *Genome Biology* **15**: 550.

780 Lucke M, Correa MG & Levy A (2020) The role of secretion systems, effectors, and secondary
781 metabolites of beneficial rhizobacteria in interactions with plants and microbes. *Frontiers in*
782 *Plant Science* **11**: 589416.

783 Luo Y, Frey EA, Pfuetzner RA, Creagh AL, Knoechel DG, Haynes CA, Finlay BB & Strynadka NCJ
784 (2000) Crystal structure of enteropathogenic *Escherichia coli* intimin–receptor complex.
785 *Nature* **405**: 1073-1077.

786 Madhaiyan M, Poonguzhali S, Senthilkumar M, Pragatheswari D, Lee J-S & Lee K-C (2015)
787 *Arachidicoccus rhizosphaerae* gen. nov., sp. nov., a plant-growth-promoting bacterium in the
788 family Chitinophagaceae isolated from rhizosphere soil. *International Journal of Systematic*
789 and *Evolutionary Microbiology* **65**: 578-586.

790 McMurdie PJ & Holmes S (2013) phyloseq: An R Package for Reproducible Interactive Analysis and
791 Graphics of Microbiome Census Data. *PLOS ONE* **8**: e61217.

792 Menzel P, Ng KL & Krogh A (2016) Fast and sensitive taxonomic classification for metagenomics with
793 Kaiju. *Nature Communications* **7**: 11257.

794 Mikryukov V (2019) metagMisc: miscellaneous functions for metagenomic analysis. *R-package*
795 Minh BQ, Schmidt HA, Chernomor O, Schrempf D, Woodhams MD, von Haeseler A & Lanfear R
796 (2020) IQ-TREE 2: New Models and Efficient Methods for Phylogenetic Inference in the
797 Genomic Era. *Molecular Biology and Evolution* **37**: 1530-1534.

798 Mistry J, Chuguransky S, Williams L, *et al.* (2020) Pfam: The protein families database in 2021. *Nucleic*
799 *Acids Research* **49**: D412-D419.

800 Nurk S, Meleshko D, Korobeynikov A & Pevzner PA (2017) metaSPAdes: a new versatile
801 metagenomic assembler. *Genome Res* **27**: 824-834.

802 Ofek-Lalzar M, Sela N, Goldman-Voronov M, Green SJ, Hadar Y & Minz D (2014) Niche and host-
803 associated functional signatures of the root surface microbiome. *Nature Communications* **5**:
804 4950.

805 Okazaki S, Okabe S, Higashi M, Shimoda Y, Sato S, Tabata S, Hashiguchi M, Akashi R, Göttfert M &
806 Saeki K (2010) Identification and functional analysis of Type III effector proteins in
807 *Mesorhizobium loti*. *Molecular Plant-Microbe Interactions* **23**: 223-234.

808 Oksanen J, Blanchet FG, Kindt R, Legendre P, Minchin PR, O'hara R, Simpson GL, Solymos P,
809 Stevens MHH & Wagner H (2013) Package ‘vegan’. *Community ecology package, version 2*:
810 1-295.

811 Parks DH, Chuvochina M, Rinke C, Mussig AJ, Chaumeil P-A & Hugenholtz P (2021) GTDB: an
812 ongoing census of bacterial and archaeal diversity through a phylogenetically consistent, rank
813 normalized and complete genome-based taxonomy. *Nucleic Acids Research* **50**: D785-D794.

814 Pascale A, Proietti S, Pantelides IS & Stringlis IA (2020) Modulation of the root microbiome by plant
815 molecules: The basis for targeted disease suppression and plant growth promotion. *Frontiers*
816 in *Plant Science* **10**: 501717.

817 Pfeilmeier S, Werz A, Ote M, Bortfeld-Miller M, Kirner P, Keppler A, Hemmerle L, Gäbelein CG,
818 Pestalozzi CM & Vorholt JA (2023) Dysbiosis of a leaf microbiome is caused by enzyme
819 secretion of opportunistic *Xanthomonas* strains. *bioRxiv* 2023.2005.2009.539948.

820 Piromyou P, Songwattana P, Boonchuen P, Nguyen HP, Manassila M, Tantanuch W, Maikhunthod B,
821 Teamtisong K, Tittabut P & Boonkerd N (2021) The new putative Type III effector SkP48 in
822 *Bradyrhizobium* sp. DOA9 is involved in legume nodulation. *Research Square* PREPRINT.

823 Poppeliers SWM, Sánchez-Gil JJ & de Jonge R (2023) Microbes to support plant health: understanding
824 bioinoculant success in complex conditions. *Current Opinion in Microbiology* **73**: 102286.

825 Putri GH, Anders S, Pyl PT, Pimanda JE & Zanini F (2022) Analysing high-throughput sequencing
826 data in Python with HTSeq 2.0. *Bioinformatics* **38**: 2943-2945.

827 R Core Team, 2020. R: A language and environment for statistical computing. R Foundation for
828 Statistical Computing, Vienna, Austria. URL <https://www.R-project.org/>

829 RStudio Team, 2019. RStudio: Integrated Development for R. RStudio, Inc., Boston, MA URL
830 <http://www.rstudio.com/>

831 Rojas-Lopez M, Zorgani MA, Kelley LA, Bailly X, Kajava AV, Henderson IR, Polticelli F, Pizza M,
832 Rosini R & Desvaux M (2018) Identification of the Autochaperone Domain in the Type Va
833 Secretion System (T5aSS): Prevalent Feature of Autotransporters with a β -Helical Passenger.
834 *Frontiers in Microbiology* **8**: 2607.

835 Rosier A, Medeiros FHV & Bais HP (2018) Defining plant growth promoting rhizobacteria molecular
836 and biochemical networks in beneficial plant-microbe interactions. *Plant and Soil* **428**: 35-55.

837 Russell Alistair B, Wexler Aaron G, Harding Brittany N, *et al.* (2014) A Type VI Secretion-Related
838 Pathway in Bacteroidetes Mediates Interbacterial Antagonism. *Cell Host & Microbe* **16**: 227-
839 236.

840 Salomon D, Kinch LN, Trudgian DC, Guo X, Klimko JA, Grishin NV, Mirzaei H & Orth K (2014)
841 Marker for type VI secretion system effectors. *Proceedings of the National Academy of
842 Sciences* **111**: 9271-9276.

843 Sánchez-Gil JJ, Poppeliers SWM, Vacheron J, Zhang H, Odijk B, Keel C & de Jonge R (2023) The
844 conserved *iol* gene cluster in *Pseudomonas* is involved in rhizosphere competence. *Current
845 Biology* **33**: 3097-3110.e3096.

846 Schneijderberg M, Cheng X, Franken C, *et al.* (2020) Quantitative comparison between the rhizosphere
847 effect of *Arabidopsis thaliana* and co-occurring plant species with a longer life history. *The
848 ISME Journal* **14**: 2433-2448.

849 Selten G, Stassen MJJ, De Rooij P, Berendsen RL, Stringlis I & de Jonge R (2024) Draft genome
850 sequences of *Arabidopsis thaliana*-associated micro-organisms from Reijerscamp soil, the
851 Netherlands [Data set]. Zenodo <https://doi.org/10.5281/zenodo.10992416>.

852 Seneviratne G, Weerasekara MLMAW, Seneviratne KACN, Zavahir JS, Kecsks ML & Kennedy IR
853 (2011) Importance of Biofilm Formation in Plant Growth Promoting Rhizobacterial Action.

854 *Plant Growth and Health Promoting Bacteria*,(Maheshwari DK, ed.) p. 81-95. Springer Berlin
855 Heidelberg, Berlin, Heidelberg.

856 Song W, Zhuang X, Tan Y, Qi Q & Lu X (2022) The type IX secretion system: Insights into its function
857 and connection to glycosylation in *Cytophaga hutchinsonii*. *Engineering Microbiology* **2**:
858 100038.

859 Staehelin C & Krishnan Hari B (2015) Nodulation outer proteins: double-edged swords of symbiotic
860 rhizobia. *Biochemical Journal* **470**: 263-274.

861 Stringlis IA, Zamioudis C, Berendsen RL, Bakker PAHM & Pieterse CMJ (2019) Type III Secretion
862 System of beneficial rhizobacteria *Pseudomonas simiae* WCS417 and *Pseudomonas defensor*
863 WCS374. *Frontiers in Microbiology* **10**: 467989.

864 Stringlis IA, Yu K, Feussner K, de Jonge R, Van Bentum S, Van Verk MC, Berendsen RL, Bakker
865 PAHM, Feussner I & Pieterse CMJ (2018) MYB72-dependent coumarin exudation shapes root
866 microbiome assembly to promote plant health. *Proceedings of the National Academy of*
867 *Sciences* **115**: E5213-E5222.

868 Suarez G, Sierra JC, Erova TE, Sha J, Horneman AJ & Chopra AK (2010) A Type VI Secretion System
869 effector protein, VgrG1, from *Aeromonas hydrophila* that induces host cell toxicity by ADP
870 ribosylation of actin. *Journal of Bacteriology* **192**: 155-168.

871 Thomas S, Holland IB & Schmitt L (2014) The Type 1 secretion pathway — The hemolysin system
872 and beyond. *Biochimica et Biophysica Acta (BBA) - Molecular Cell Research* **1843**: 1629-1641.

873 Verster AJ, Ross BD, Radey MC, Bao Y, Goodman AL, Mougous JD & Borenstein E (2017) The
874 landscape of Type VI Secretion across human gut microbiomes reveals its role in community
875 composition. *Cell Host & Microbe* **22**: 411-419.e414.

876 Vogel CM, Potthoff DB, Schäfer M, Barandun N & Vorholt JA (2021) Protective role of the
877 *Arabidopsis* leaf microbiota against a bacterial pathogen. *Nature Microbiology* **6**: 1537-1548.

878 von Meijenfeldt FAB, Arkhipova K, Cambuy DD, Coutinho FH & Dutilh BE (2019) Robust taxonomic
879 classification of uncharted microbial sequences and bins with CAT and BAT. *Genome Biology*
880 **20**: 217.

881 Wallner A, Moulin L, Busset N, Rimbault I & Béna G (2021) Genetic diversity of Type 3 Secretion
882 System in *Burkholderia* s.l. and links with plant host adaptation. *Frontiers in Microbiology* **12**:
883 761215.

884 Wang J, Ma C, Ma S, *et al.* (2022) GmARP is related to the Type III effector NopAA to promote
885 nodulation in soybean (*Glycine max*). *Frontiers in Genetics* **13**: 889795.

886 Wattam AR, Davis JJ, Assaf R, *et al.* (2017) Improvements to PATRIC, the all-bacterial Bioinformatics
887 Database and Analysis Resource Center. *Nucleic Acids Res* **45**: D535-d542.

888 Wen T, Yuan J, He X, Lin Y, Huang Q & Shen Q (2020) Enrichment of beneficial cucumber
889 rhizosphere microbes mediated by organic acid secretion. *Horticulture Research* **7**: 154.

890 Wilhelm S, Rosenau F, Kolmar H & Jaeger K-E (2011) Autotransporters with GDSL passenger
891 domains: Molecular physiology and biotechnological applications. *ChemBioChem* **12**: 1476-
892 1485.

893 Willett JLE, Ruhe ZC, Goulding CW, Low DA & Hayes CS (2015) Contact-dependent growth
894 inhibition (CDI) and CdiB/CdiA two-partner secretion proteins. *Journal of Molecular Biology*
895 **427**: 3754-3765.

896 Wood DE, Lu J & Langmead B (2019) Improved metagenomic analysis with Kraken 2. *Genome
897 Biology* **20**: 257.

898 Xu J, Zhang Y, Zhang P, *et al.* (2018) The structure and function of the global citrus rhizosphere
899 microbiome. *Nature Communications* **9**: 4894.

900 Xu L, Dong Z, Chiniquy D, *et al.* (2021) Genome-resolved metagenomics reveals role of iron
901 metabolism in drought-induced rhizosphere microbiome dynamics. *Nature Communications*
902 **12**: 3209.

903 Ye T, Zhou T, Li Q, Xu X, Fan X, Zhang L & Chen S (2020) *Cupriavidus* sp. HN-2, a Novel Quorum
904 Quenching Bacterial Isolate, is a Potent Biocontrol Agent Against *Xanthomonas campestris* pv.
905 *campestris*. *Microorganisms* **8**: 45.

906 Yu P, He X, Baer M, *et al.* (2021) Plant flavones enrich rhizosphere Oxalobacteraceae to improve maize
907 performance under nitrogen deprivation. *Nature Plants* **7**: 481-499.

908 Zboralski A, Biessy A & Filion M (2022) Bridging the gap: Type III Secretion Systems in plant-
909 beneficial bacteria. *Microorganisms* **10**: 187.

910 Zeng C & Zou L (2017) An account of in silico identification tools of secreted effector proteins in
911 bacteria and future challenges. *Briefings in Bioinformatics* **20**: 110-129.

912 Zhao X, Wang Y, Shang Q, Li Y, Hao H, Zhang Y, Guo Z, Yang G, Xie Z & Wang R (2015) Collagen-
913 like proteins (ClpA, ClpB, ClpC, and ClpD) are required for biofilm formation and adhesion to
914 plant roots by *Bacillus amyloliquefaciens* FZB42. *PLOS ONE* **10**: e0117414.

915 Zhou Y, Coventry DR, Gupta VVSR, *et al.* (2020) The preceding root system drives the composition
916 and function of the rhizosphere microbiome. *Genome Biology* **21**: 89.

917

Figures

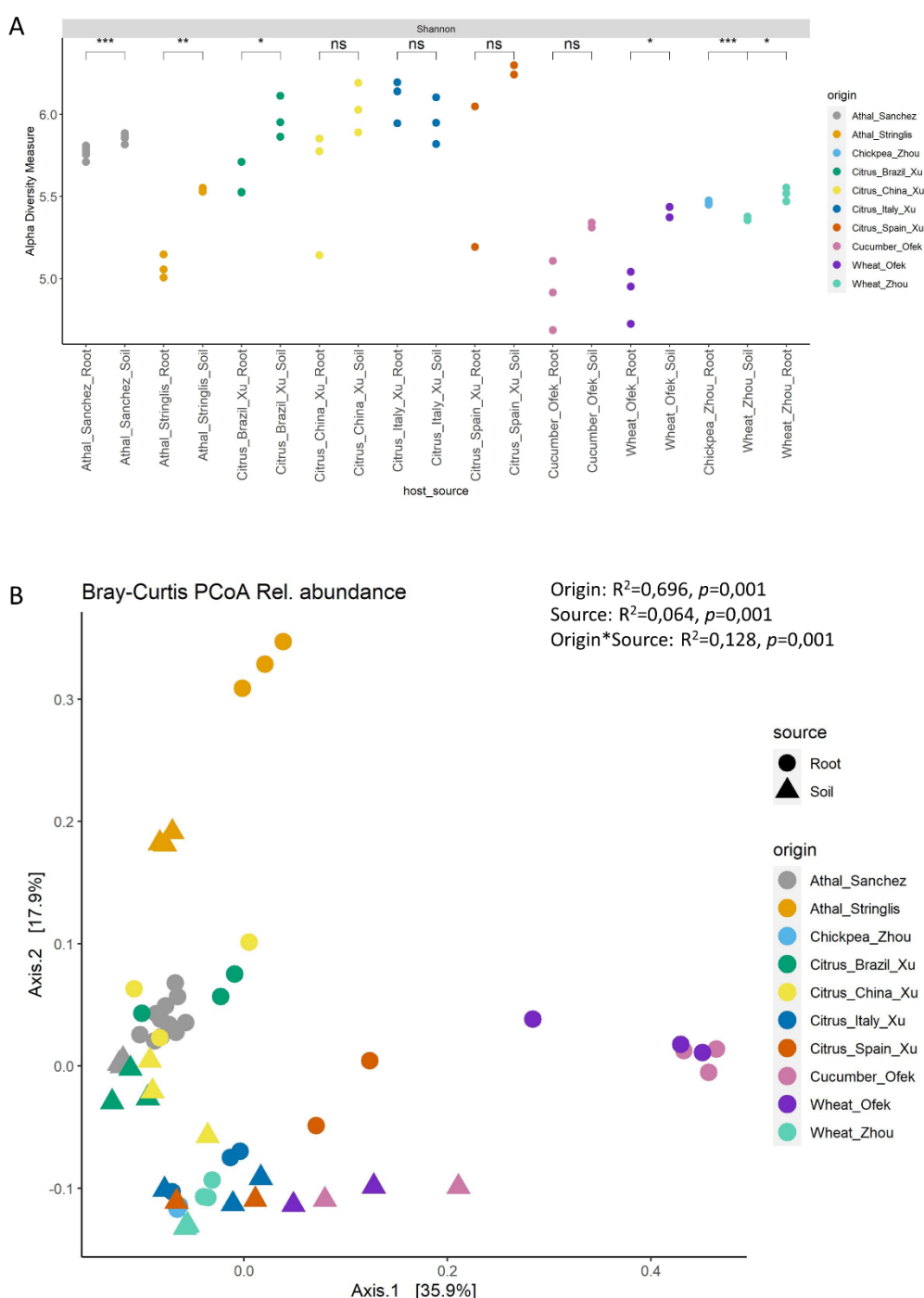


Figure 1. Alpha- and beta diversity of all metagenomic datasets, based on genus rank classification of metagenomic reads (Kaiju). A) The Shannon-diversity index was compared between the rhizosphere and soil samples of each plant species to determine the rhizosphere effect (lower diversity in the rhizosphere) in each study. Studies with significant differences (t-test, p value < 0.05 , BH-correction) are indicated with an asterisk. B) Pairwise sample-to-sample Bray-Curtis dissimilarities were used to perform principal coordinate analysis (based on genera $> 1 \cdot 10^{-5}$ relative abundance) to illustrate differences in community composition between plant species and different biomes (rhizosphere vs soil).

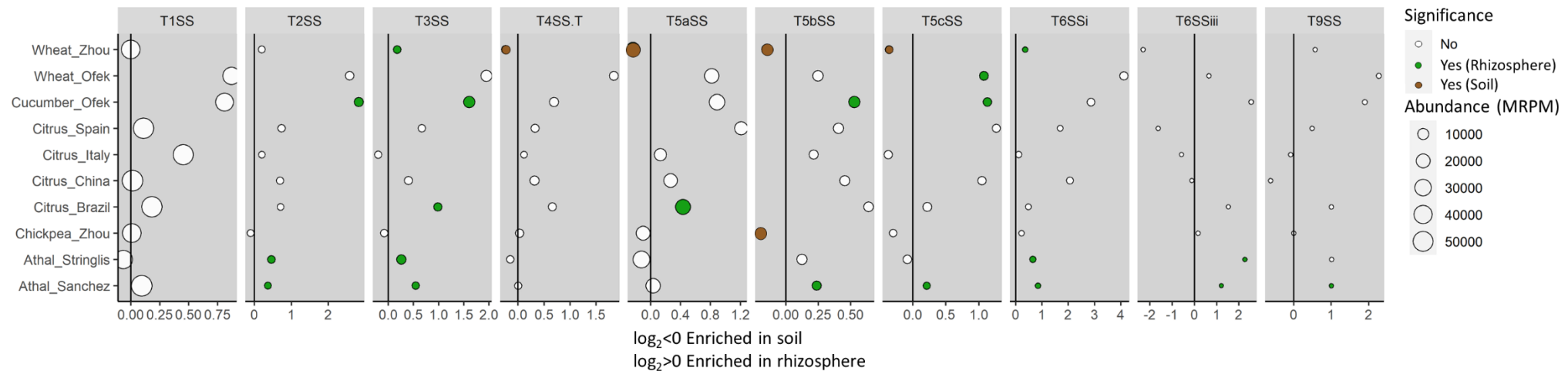


Figure 2. Secretion systems enriched in the rhizosphere or soil in each plant species. Green and brown circles indicate SS's that were significantly more abundant in one of the biomes (t-test, p value <0.05 , BH-correction). Some SS's were more abundant in a specific biome but not significantly so, mostly due to the variation between samples in a dataset. The abundance in the rhizosphere relative to the soil is indicated on the x-axis as log-fold values (positive enriched in rhizosphere, negative enriched in soil) and circle sizes represent the MRPM abundance of the SS in a plant dataset.

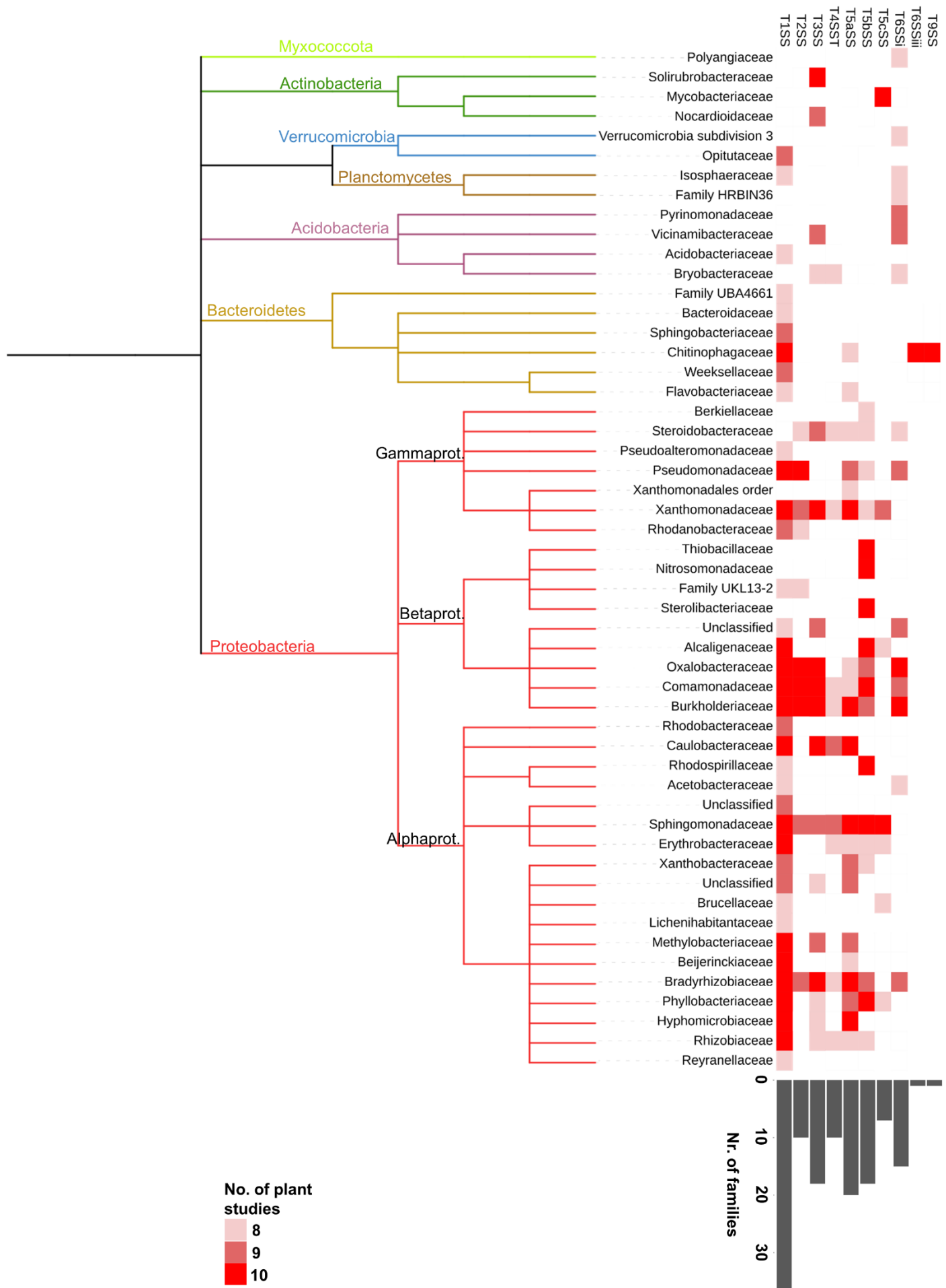


Figure 3. Fifty-two bacterial families encoding SS's in the rhizosphere (detected in $\geq 80\%$ of the plant studies/datasets). The coloured gradient boxes relate to the number of plant studies in which a family with the corresponding SS was detected (8-10 studies). Some families were detected in all studies considered (dark red). The bar plot at the bottom summarises the total number of families in which a SS was observed.

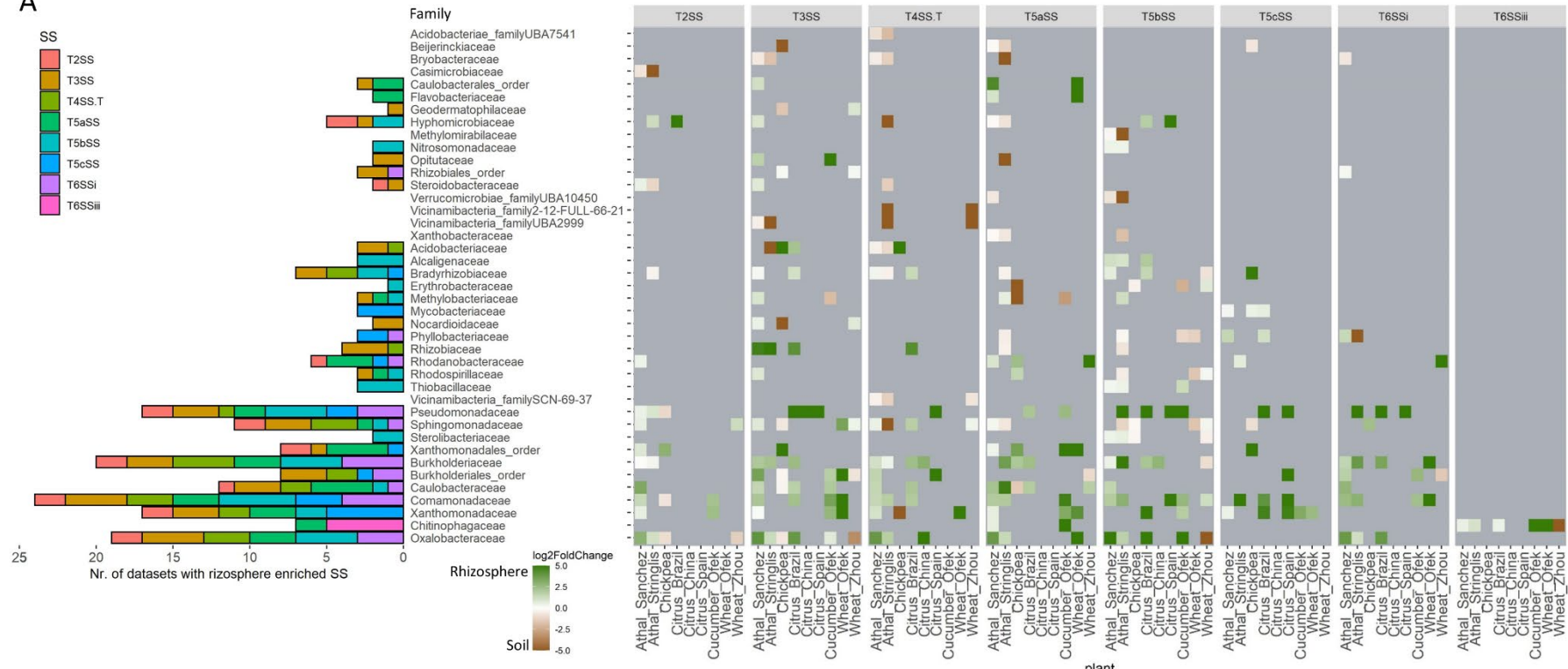
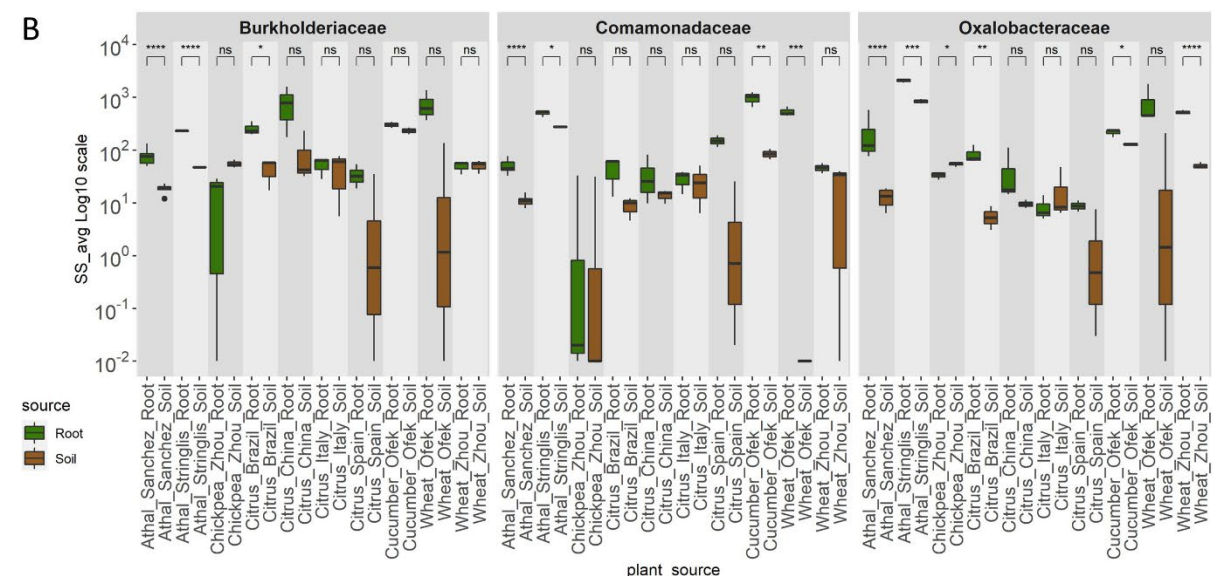
A**B**

Figure 4. Enrichment of SS's of specific families in all plant studies/datasets investigated. A) The \log_2 fold difference ranges from green (enriched in the rhizosphere) to brown (enriched in the soil). Families that showed a significant enrichment in rhizosphere or soil for a specific SS in more than one dataset is displayed, starting with the families present in most datasets from the bottom of the figure. The counts of SS's per family is summarised on the left in a barplot. B) Three prominent families, *Oxalobacteriaceae*, *Burkholderiales* and *Comamonadaceae*, showed enrichment of the T3SS in multiple datasets. The \log_{10} (MRPM abundance) of the T3SS is shown for the rhizosphere and soil biomes across the different studies and plants.

T6SS Phylogenetic cluster

- Group 2
- Group 3
- Group 4A
- Group 4B

Family

- Burkholderiaceae
- Comamonadaceae
- Oxalobacteraceae

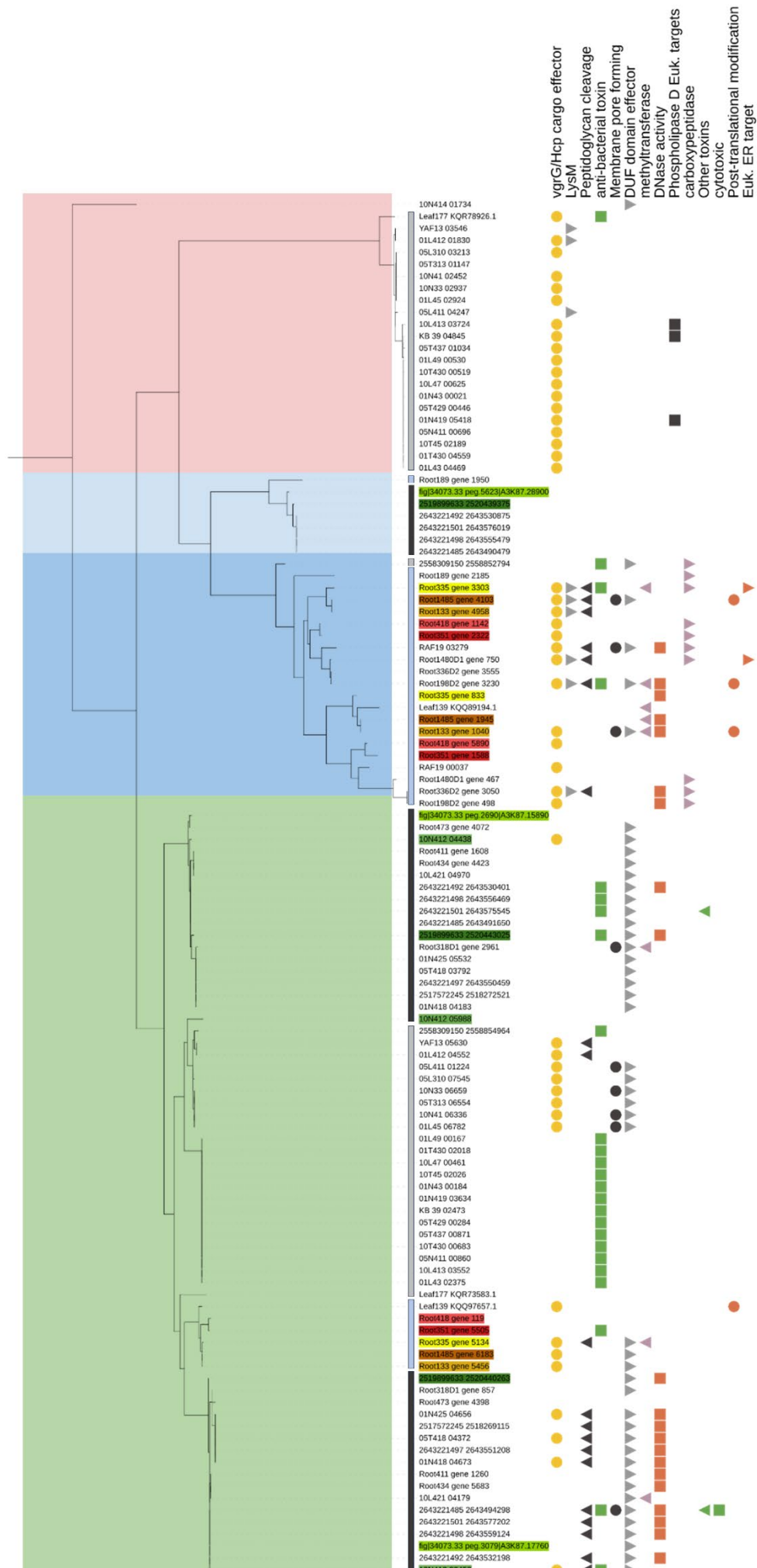


Figure 5. Summary of isolates encoding two or three T6SS copies in their genomes. Different effector functions can be linked to the different copies of T6SS's. The ML tree was constructed based on the *tssB* gene. Coloured ranges on the branches indicate the well-known T6SS taxonomic groups. Coloured strips before the labels (gray scales) indicate taxonomic identity. Isolates with three T6SS copies are highlighted with coloured labels, each colour corresponding to a single genome. The different effector functions are summarised by the different coloured shapes.

Supplementary figures

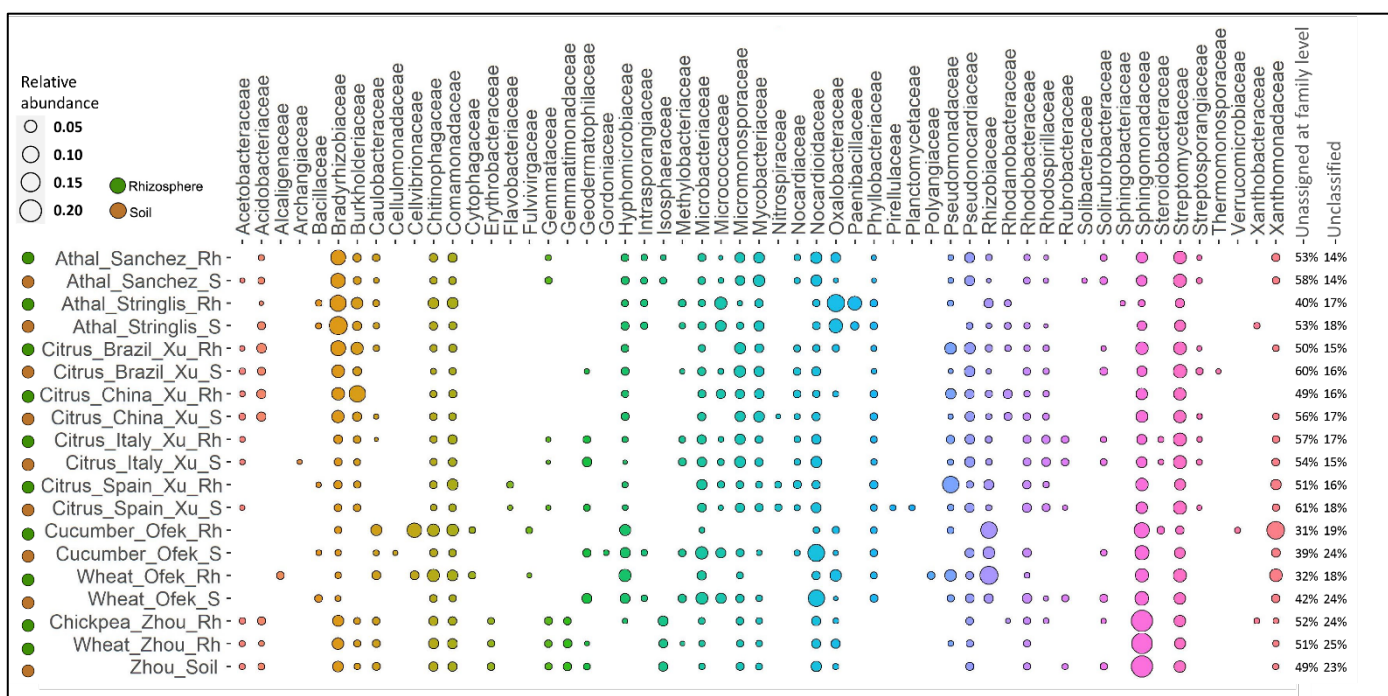


Figure S1. Families with > 1% relative abundance in the classified bacterial reads of the metagenomes of the different plant species (Kaiju read classification). Some plants had clear distinctions between rhizosphere (Rh) and soil (S), while others were highly similar in both biomes. Some of the most abundant families in all plants were *Bradyrhizobiaceae*, *Burkholderiaceae*, *Sphingomonadaceae* and *Streptomycetaceae*.

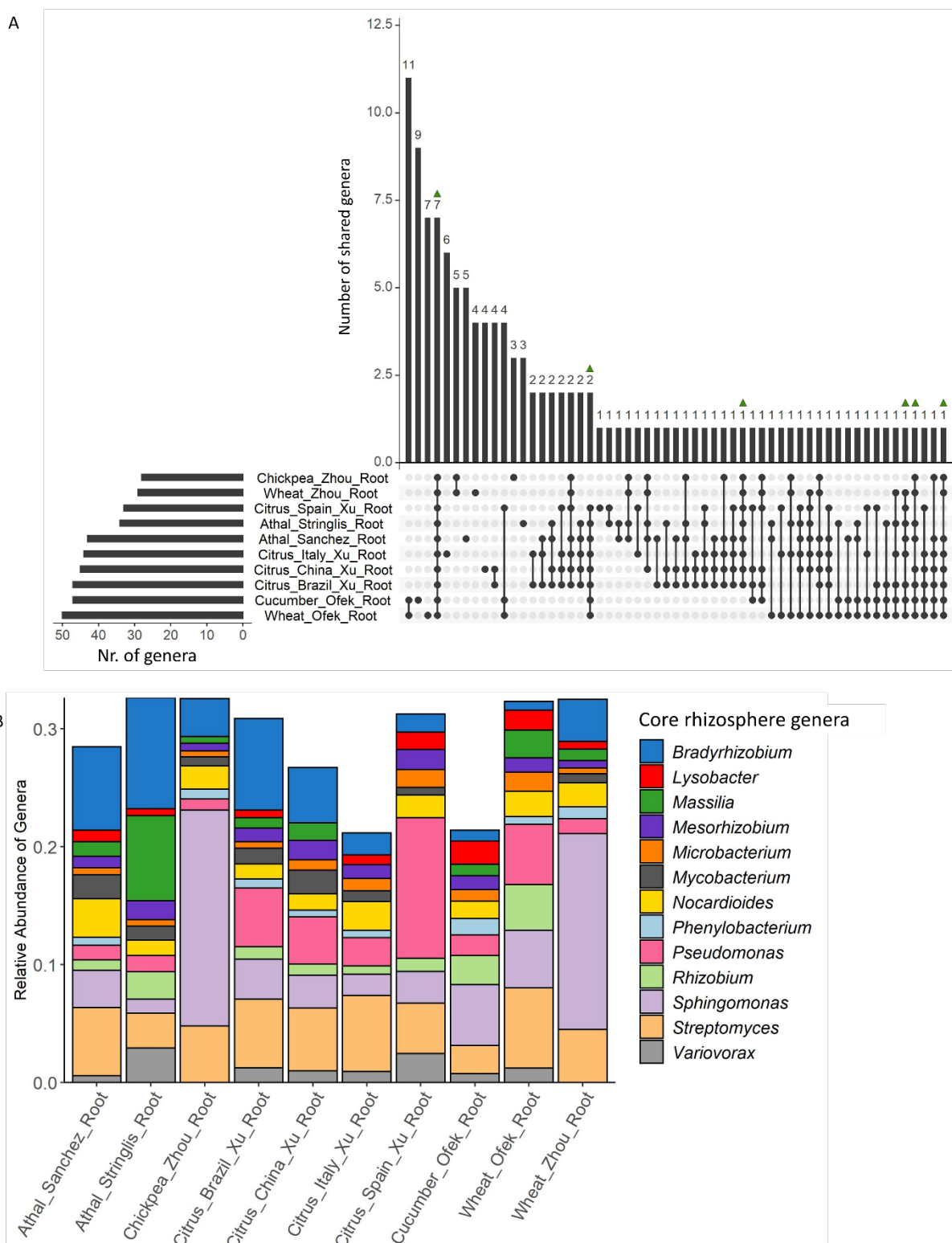
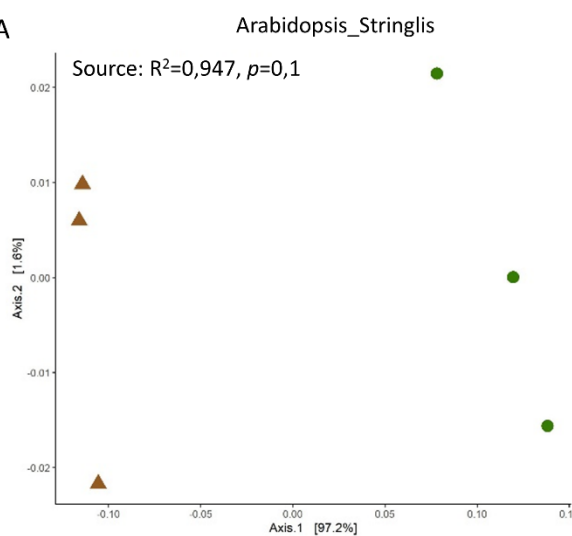
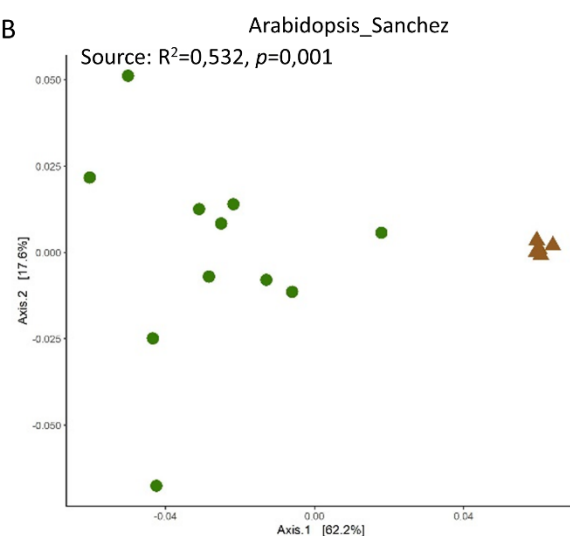


Figure S2. Summary of core bacterial genera (> 0.5% relative abundance) in the rhizosphere of all plant datasets, based on all bacterial reads classified at genus rank (Kaiju). A) The number of core genera and genera unique to each study is shown by connected dots. Green triangles indicate the genera present in >80% of all rhizosphere datasets (core genera) B) The relative abundance of the 13 core genera in the rhizospheres of the different datasets are illustrated in the coloured bar graph.

A



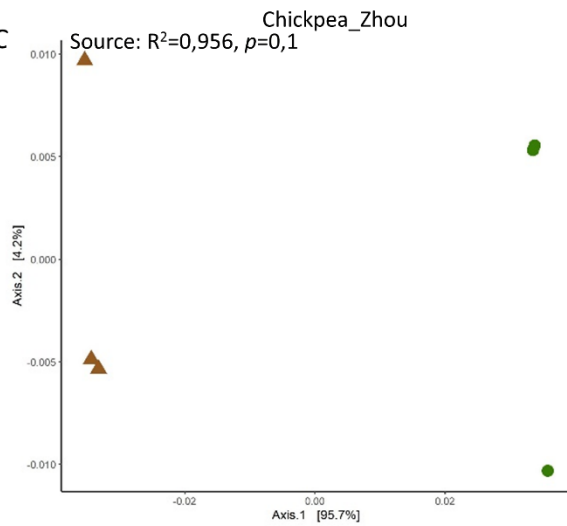
B



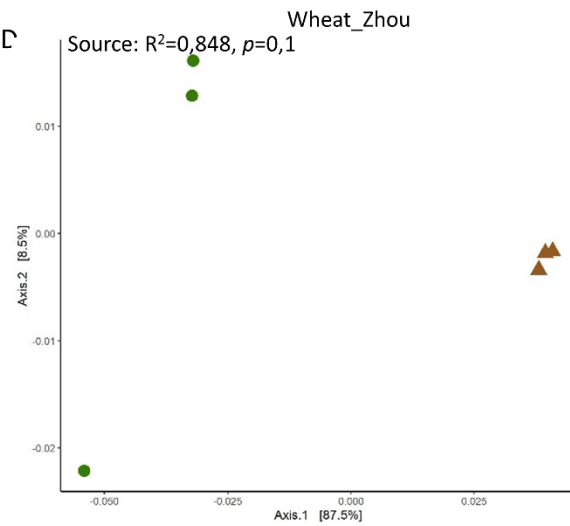
Source

Root
Soil

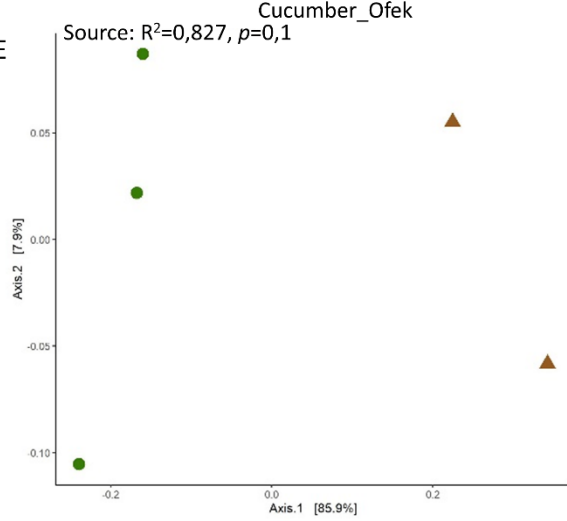
C



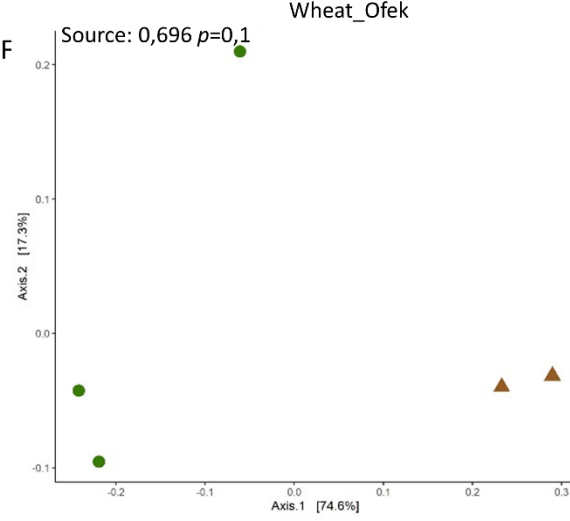
D



E



F



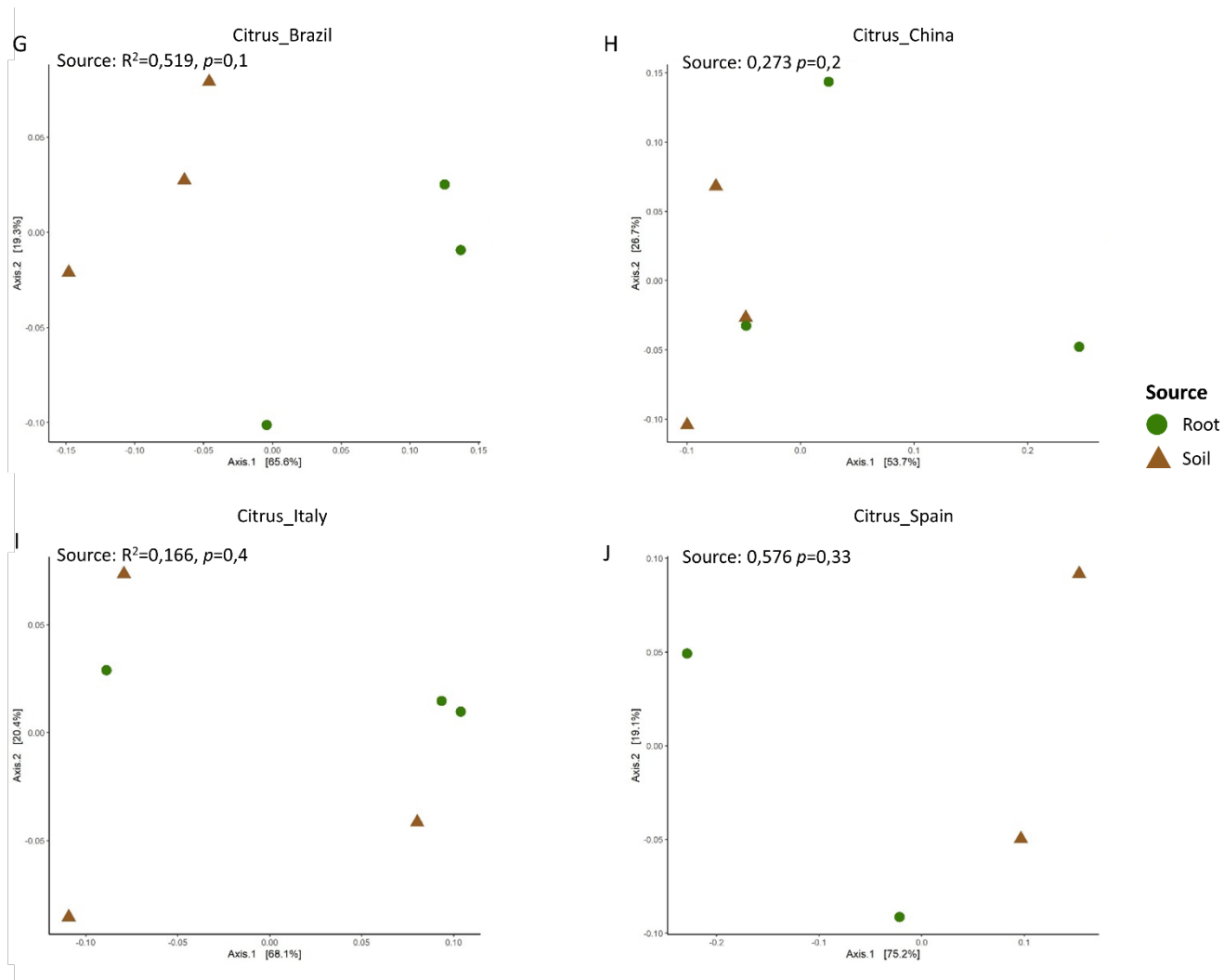


Figure S3. Dataset-specific beta-diversity analyses. The Bray-Curtis distances between samples were used to construct a principal coordinate analysis plot (based on genera $> 1e-5$ relative abundance) to illustrate differences in community composition between rhizosphere and soil in each dataset, including A) *Arabidopsis_Stringlis*, B) *Arabidopsis_Sanchez*, C) *Chickpea_Zhou*, D) *Wheat_Zhou*, E) *Cucumber_Ofek*, F) *Wheat_Ofek*, G) *Citrus_Brazil*, H) *Citrus_China*, I) *Citrus_Italy*, J) *Citrus_Spain*

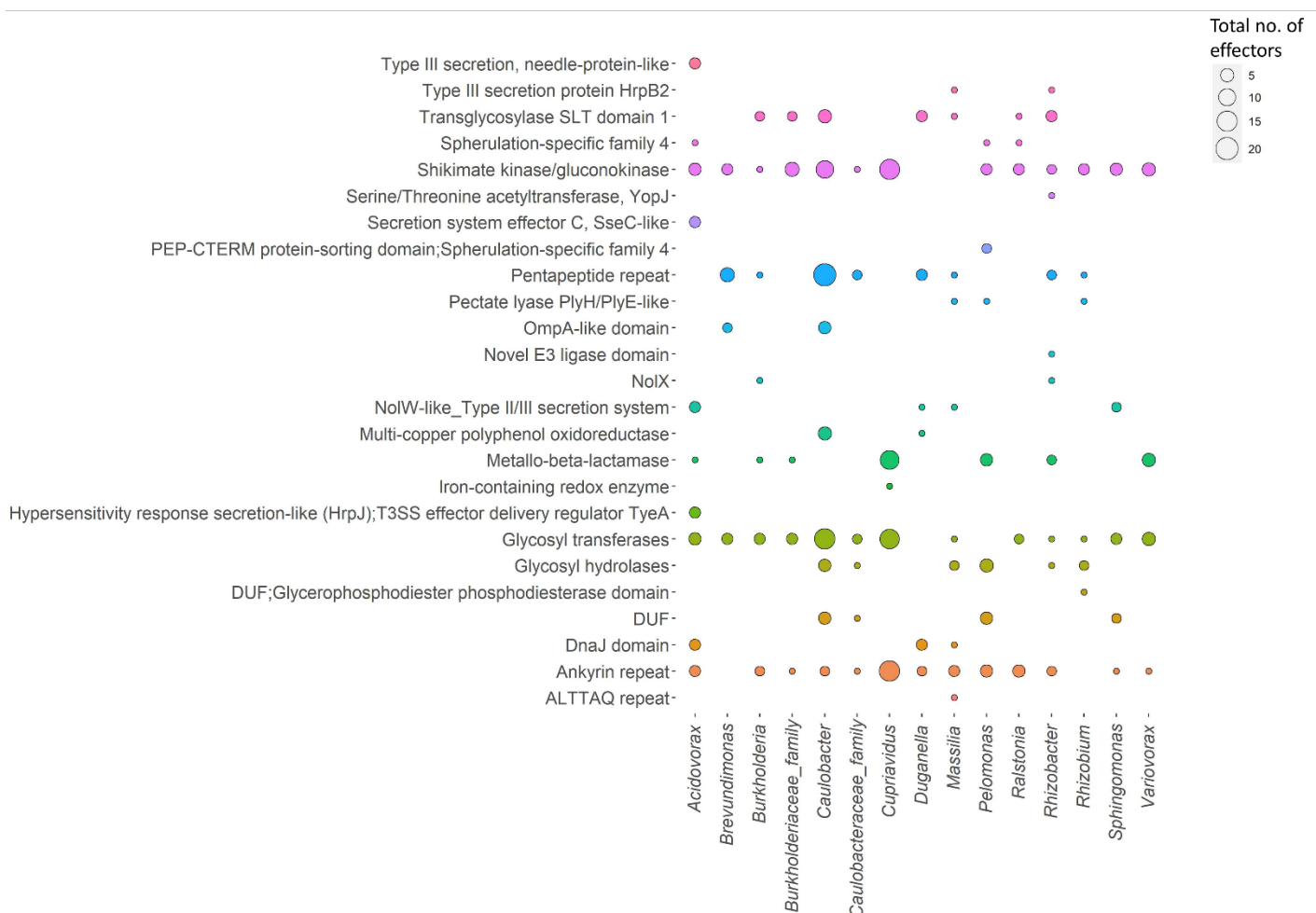


Figure S4. Summary of the functional T3SS effector domains present in different genera of the *A. thaliana* isolated bacterial genomes. Dot sizes represent the number of effectors predicted in the genus and the colours correspond to the functional domains.

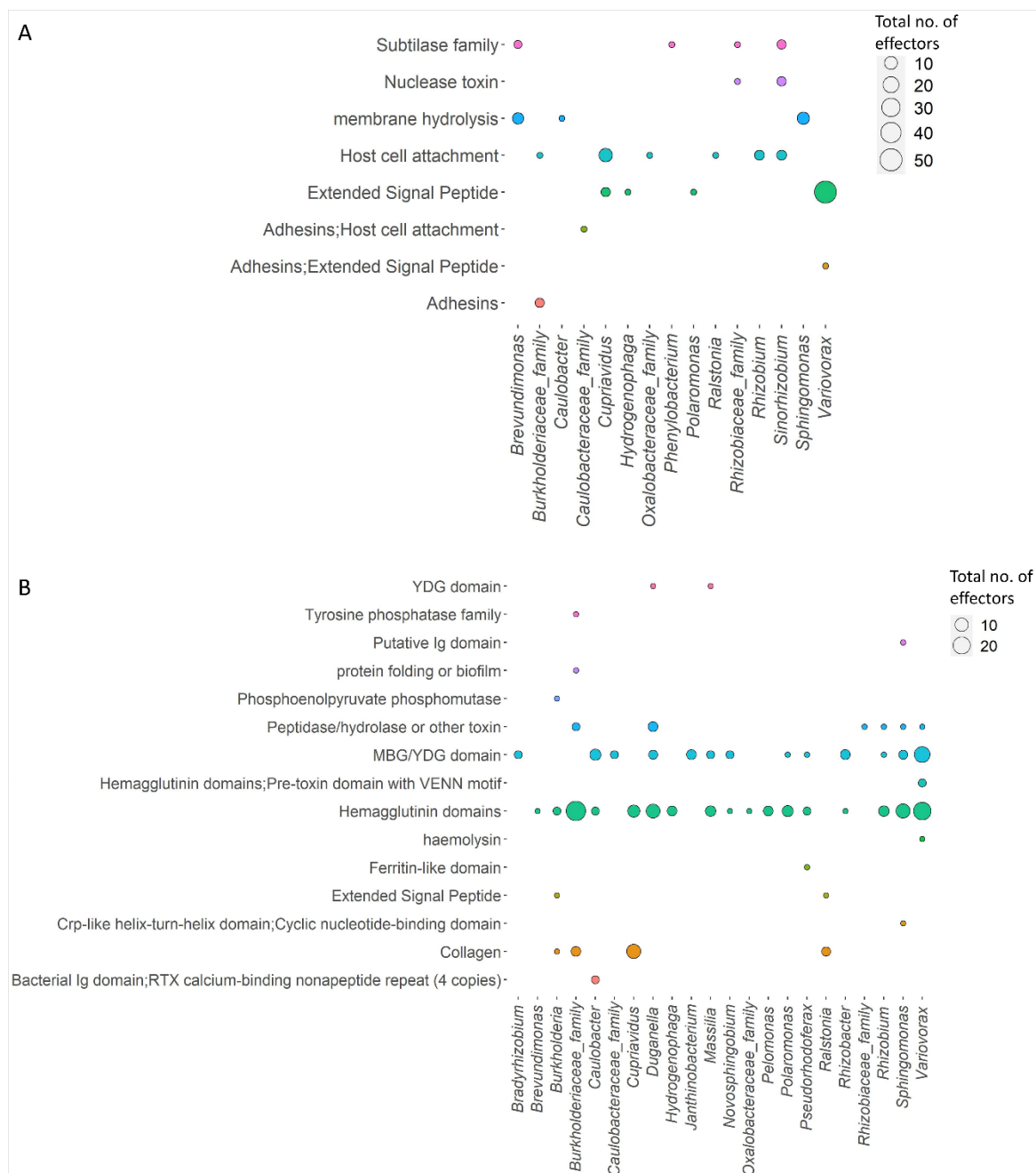


Figure S5. Summary of the functional domains/categories identified for the T5SS effectors, indicating the abundance of the categories in the (A) T5aSS and (B) T5bSS. Dot sizes represent the number of effectors predicted in the genus and the colours correspond to the functional domains.

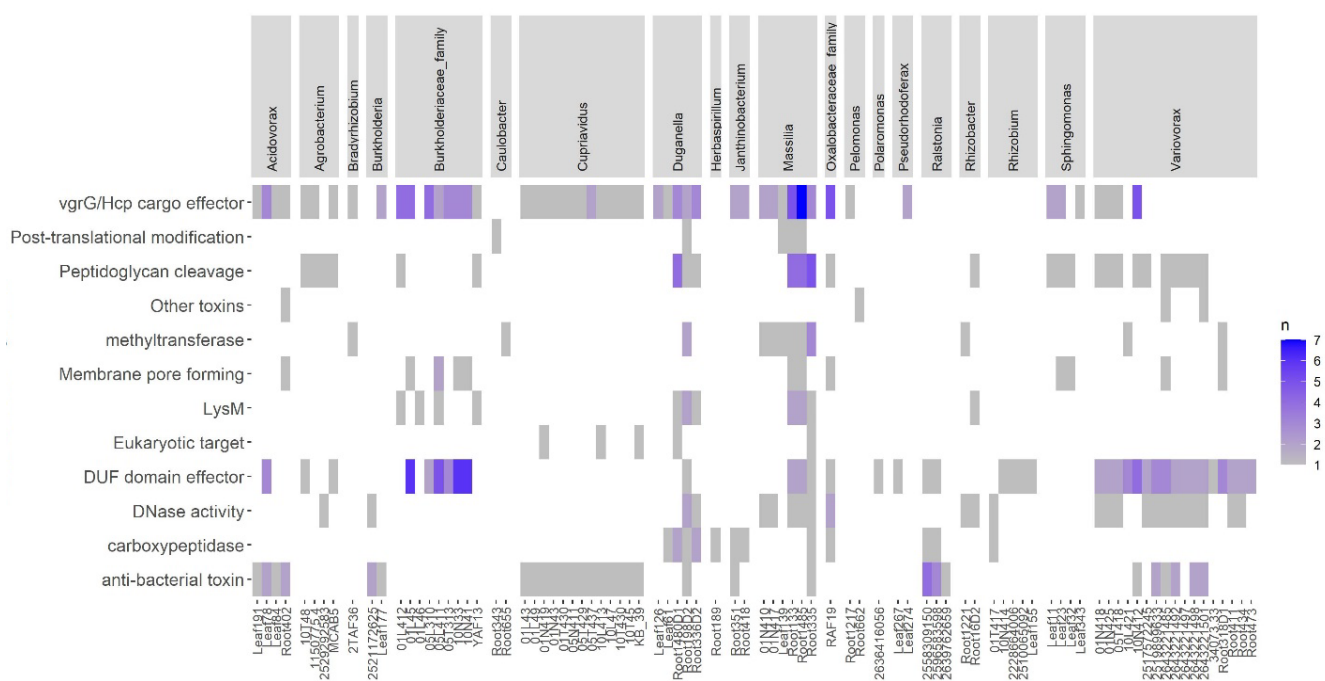


Figure S6. Summary of the effector functions identified in families with a T6SS and enriched in the rhizosphere.

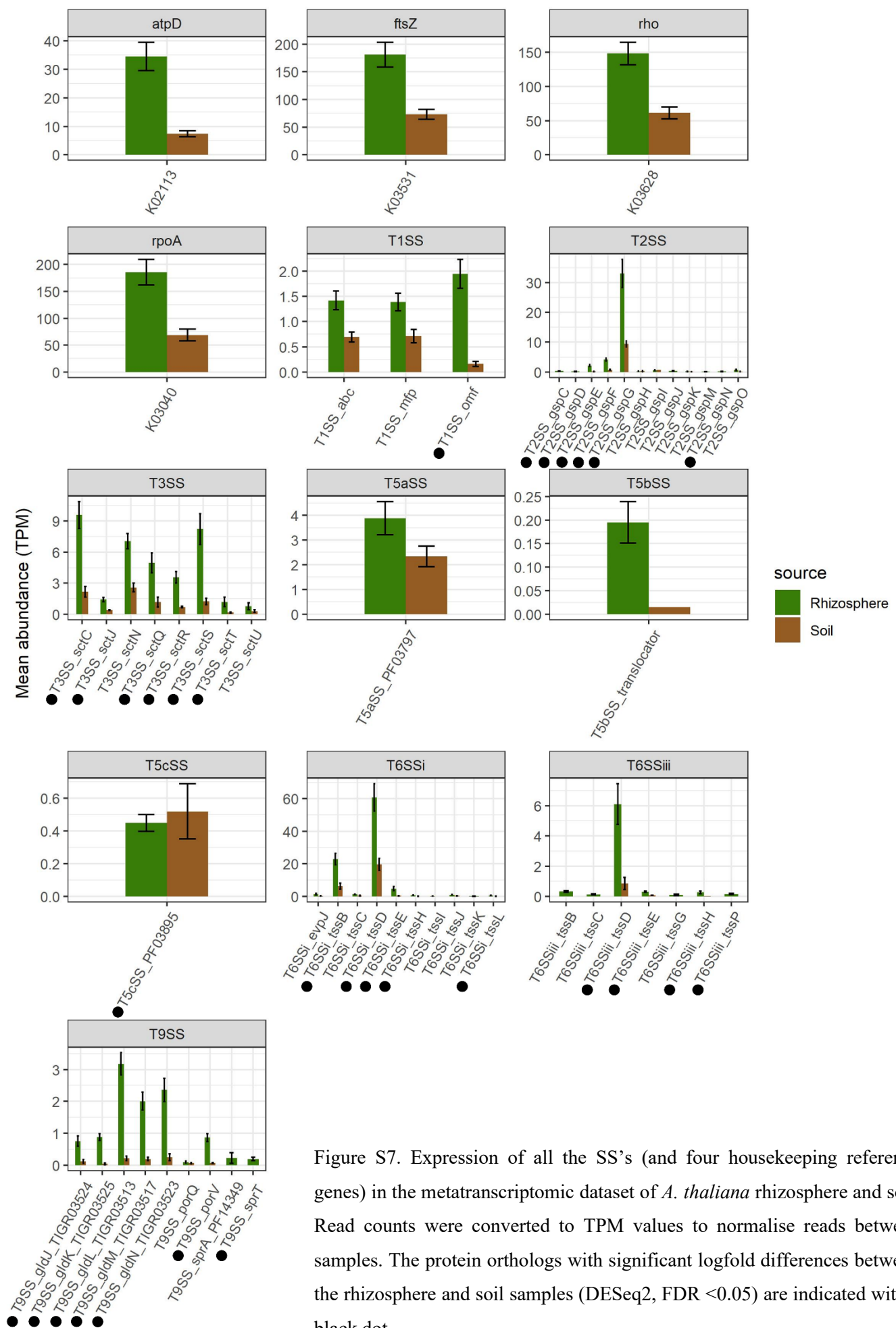


Figure S7. Expression of all the SS's (and four housekeeping reference genes) in the metatranscriptomic dataset of *A. thaliana* rhizosphere and soil. Read counts were converted to TPM values to normalise reads between samples. The protein orthologs with significant logfold differences between the rhizosphere and soil samples (DESeq2, FDR < 0.05) are indicated with a black dot.